

Analytic potentials and vibrational energies for Li_2 states dissociating to $\text{Li}(2S) + \text{Li}(3P)$. Part 1: The $^{2S+1}\Pi_{u/g}$ states

Nikesh S. Dattani,*

¹*School of Materials Science and Engineering, Nanyang Technological University, 639798, Singapore,*

²*Fukui Institute for Fundamental Chemistry, 606-8103, Kyoto, Japan, and*

³*Quantum Chemistry Laboratory, Department of Chemistry, Kyoto University, 606-8502, Kyoto, Japan,*

Analytic potentials are built for all four $^{2S+1}\Pi_{u/g}$ states of Li_2 dissociating to $\text{Li}(2S) + \text{Li}(3P)$: $3b(3^3\Pi_u)$, $3B(3^1\Pi_u)$, $3C(3^1\Pi_g)$, and $3d(3^3\Pi_g)$. These potentials include the effect of spin-orbit coupling for large internuclear distances, and include state of the art long-range constants. This is the first successful demonstration of fully analytic diatomic potentials that capture features that are usually considered too difficult to capture without a point-wise potential, such as multiple minima, and shelves. Vibrational energies for each potential are presented for the isotopologues $^6,^6\text{Li}_2$, $^6,^7\text{Li}_2$, $^7,^7\text{Li}_2$, and the elusive ‘halo nucleonic molecule’ $^{11,11}\text{Li}_2$. These energies are claimed to be accurate enough for new high-precision experimental setups such as the one presented in [Sebastian *et al.* Phys. Rev. A, **90**, 033417 (2014)] to measure and assign energy levels of these electronic states, all of which have not yet been explored in the long-range region. Measuring energies in the long-range region of these electronic states may be significant for studying the *ab initio* vs experiment discrepancy discussed in [Tang *et al.* Phys. Rev. A, **84**, 052502 (2014)] for the C_3 long-range constant of Lithium, which has significance for improving the SI definition of the second.

PACS numbers: 02.60.Ed , 31.50.Bc , 82.80.-d , 31.15.ac, 33.20.-t , 82.90.+j, 97 , 98.38.-j , 95.30.Ky

Very little is known about the Li_2 electronic states dissociating to the $2S + 3P$ asymptote. Out of the first 5 asymptotes (from lowest to highest: $2S + 2S$, $2S + 2P$, $2S + 3S$, $2P + 2P$ and $2S + 3P$), the $2S + 3P$ is the only one for which an empirical dissociation energy has not been determined for any of the electronic states dissociating to it. Furthermore, the only measurements that have been made for electronic states dissociating to $2S + 3P$, were for the $3c(3^3\Sigma_g^+)$ state [1–3] the $6X(6^1\Sigma_g^+)$ state [4, 5], and the $3d(3^3\Pi_g)$ state [6–9]. No measurements have been done on the other states dissociating to $2S + 3P$.

Very recently, a promising experiment has been setup with the ability to use photoassociation in a magneto-optical trap to make ultra-cold $^6\text{Li}_2$ molecules dissociating to the $2S + 3P$ asymptote [10], much like slightly earlier experiments which have already been successful for creating ultra-cold $^6\text{Li}_2$ molecules dissociating to $2S + 2P$ with very similar techniques [11, 12]. Measurements of the binding energies for levels very close to the $2S + 3P$ asymptote would allow for an empirical determination of the long-range constant C_3^{2S+3P} which is the leading interaction constant in the potential energy between $\text{Li}(2S)$ and $\text{Li}(3P)$.

At the lower asymptote of $2S + 2P$, there is a discrepancy between experiment and theory for the long-range constant C_3^{2S+2P} , despite Li only having $3e^-$ and the experimental value being the most precisely determined oscillator strength ever determined for a molecule, by an order of magnitude [13]. This has various consequences, reaching as far as limiting progress towards improving

the precision of the SI definition of the second [14]. More precise atomic clocks are needed for various applications. The current definition of the second is based on a clock transition frequency in Cs with a relative uncertainty of $\sim 5 \times 10^{-16}$, and a commonly quoted target for improved precision is 10^{-18} [14]. The largest source of uncertainty limiting atomic clock precision is the blackbody radiation shift, which depends on the static dipole polarizability of the system being used for the atomic clock [14]. Lithium is expected to play a major role in polarizability metrology, since polarizability ratios can be measured much more precisely than individual polarizabilities [15] and Li is the preferred choice for the standard in the denominator of such a ratio [14]. The discrepancy in C_3 limits the accuracy of a potential Li-based standard for polarizabilities [13], and hence indirectly impacts progress towards improving the SI definition of the second.

Regarding the empirical value for C_3^{2S+2P} , for most electronic states, the mixing of various states towards the $2S + 2P$ asymptote significantly complicates the expressions from which C_3 is fitted [16–20]. The complicated expressions for this mixing are the same at the $2S + 3P$ asymptote as they are for the $2S + 2P$ asymptote [21], but the fine structure splitting parameter which governs the significance of this mixing, is about 3.5 times smaller at the $2S + 3P$ asymptote than at the $2S + 2P$ asymptote. For $2S + 2P$ the fine structure splitting parameter for ^6Li is $\Delta E_{2^2P_{3/2} \leftarrow 2^2P_{1/2}} = D_2 - D_1 = 0.3353246 \text{ cm}^{-1}$ [11, 12, 22, 23], while for $2S + 3P$ it is only $\Delta E_{3^2P_{3/2} \leftarrow 3^2P_{1/2}} = 0.096 \text{ cm}^{-1}$ [24]. Therefore, C_3^{2S+3P} might be a better benchmark for an *ab initio* vs experiment comparison than C_3^{2S+2P} , as the effect of this complication is smaller.

* dattani.nike@gmail.com

$$u^{3b}(r) = \begin{cases} u^{3b,0_u^+}(r) \xrightarrow{u^{6A,0_u^+}(r)} 2S_{1/2} + 3P_{1/2} \text{ (higher)} \\ u^{3b,0_u^-}(r) \xrightarrow{u^{6a,0_u^-}(r)} 2S_{1/2} + 3P_{3/2} \text{ (lower)} \\ u^{3b,1_u}(r) \xrightarrow{u^{3B,1_u}(r), u^{6a,1_u}(r)} 2S_{1/2} + 3P_{3/2} \text{ (lowest)} \\ u^{3b,2_u}(r) \xrightarrow{\hspace{2cm}} 2S_{1/2} + 3P_{3/2} \end{cases}$$

$$u^{3B}(r) = u^{3B,1_u}(r) \xrightarrow{u^{6a,1_u}(r), u^{3b,1_u}(r)} 2S_{1/2} + 3P_{3/2} \text{ (middle)}$$

$$u^{3C}(r) = u^{3C,1_g}(r) \xrightarrow{u^{3c,1_g}(r), u^{3d,1_g}(r)} 2S_{1/2} + 3P_{3/2} \text{ (middle)}$$

$$u^{3d}(r) = \begin{cases} u^{3d,0_g^+}(r) \xrightarrow{u^{6X,0_g^+}(r)} 2S_{1/2} + 3P_{1/2} \text{ (lower)} \\ u^{3d,0_g^-}(r) \xrightarrow{u^{3c,0_g^-}(r)} 2S_{1/2} + 3P_{3/2} \text{ (higher)} \\ u^{3d,1_g}(r) \xrightarrow{u^{3c,1_g}(r), u^{3C,1_g}(r)} 2S_{1/2} + 3P_{3/2} \text{ (highest)} \\ u^{3d,2_g}(r) \xrightarrow{\hspace{2cm}} 2S_{1/2} + 3P_{3/2} \end{cases}$$

Measuring and assigning molecular energy levels using photoassociation requires reasonably accurate predictions which come from eigenvalues of a Schrödinger equation, and hence require a reasonably accurate potential energy surface. Due to the shortage of measurements on the Li_2 $2S^{+1}\Pi_{u/g}$ states dissociating to $2S + 3P$, the most accurate potentials come from purely *ab initio* calculations. For the $3c(3^3\Sigma_g^+)$ and $3A(3^1\Sigma_u^+)$ states, *ab initio* calculations were reported in 1985 [25], 1995 [26], 2006 [27] and 2014 [28, 29]; and for the $3d(3^3\Pi_g)$ state in 1995 [6] and 2014 [28, 29]. But for the rest of the states dissociating to $2S + 3P$; namely $3b(3^3\Pi_u)$, $6X(6^1\Sigma_g^+)$, $3B(3^1\Pi_u)$, $3C(3^1\Pi_g)$, and $6a(6^3\Sigma_u^+)$; the only *ab initio* calculations reported were in [26, 28, 29]. All of these *ab initio* papers also reported potentials for states dissociating to lower asymptotes, where plenty of experimental data is available to gauge the quality of the calculations.

In my very recent paper on comparing experiment to *ab initio* for the $b(1^3\Pi_u)$ state [16], it was found that the *ab initio* potential of [28] predicted all vibrational binding energies with a disagreement of $< 12 \text{ cm}^{-1}$ with the corresponding energies of the empirical potential. Furthermore there was always $< 0.8 \text{ cm}^{-1}$ disagreement between the empirical and *ab initio* vibrational energy spacings. Finally, when comparing the dissociation energies \mathcal{D}_e from [28] to the corresponding experimental values for all states which have empirical \mathcal{D}_e values available, the *ab initio* values from [28] were never in disagreement by more than 68 cm^{-1} . Therefore, the *ab initio* potentials from [28] for the states dissociating to $2S + 3P$ are expected to be a good starting point for predicting energy

levels with the precision required for photoassociation experiments as in [11, 12] and as may be performed with the new setup in [10] which is capable of detecting states dissociating to $2S + 3P$.

However, the *ab initio* calculations of [28] still have some major drawbacks (including, but not limited to):

1. the *ab initio* points are not on a dense enough mesh to use as the mesh for solving the effective radial Schrödinger equation for predicting the vibrational energies (*especially* for large distances where the energies become more important for fitting an empirical C_3 value, and for experiments such as those potentially resulting from a setup such as in [10]);
2. the *ab initio* points neglect the effect of spin-orbit coupling, which is particularly important for $nS + n'P$ states of Li_2 , where the effect of interstate coupling has been shown to be absolutely obligatory for describing the high vibrational energy measurements [11, 12, 17, 18];
3. the *ab initio* points do not go beyond the Born-Oppenheimer approximation (so do not distinguish between different isotopologues such as ${}^6,6\text{Li}_2$, ${}^6,7\text{Li}_2$, ${}^7,7\text{Li}_2$, and the elusive ‘halo nucleonic’ isotopologues containing ${}^{11}\text{Li}$), and they are non-relativistic.

Drawback (1) is usually treated by fitting an interpolant through the *ab initio* points, but the resulting energies predicted after solving the Schrödinger equation, will be very sensitive to the type of interpolant used, especially

at the level of precision of photoassociation experiments (the precision in the Li_2 measurements of [11, 12] was $\pm 0.00002 \text{ cm}^{-1}$ or $\pm 600 \text{ kHz}$). Also, if for sake of ease, a spline interpolant is used, it would be defined piecewise and would have discontinuous first derivatives. The spline also knows nothing about the physics of nature, and will therefore not know what to do in regions where fewer *ab initio* points are available (in this example, for large internuclear distances).

Rather than interpolating with a spline, we can fit to a fully analytic model potential that has the correct theoretical behavior incorporated in the long-range region where fewer *ab initio* points are available, and this addresses drawback (2) as well, since the effect of spin-orbit coupling at long-range can easily be incorporated into the model. Part of drawback (3) can also be addressed by fitting to a model potential, because the model can also build in some types of relativistic effects such as QED retardation, as was attempted in [11, 12, 17, 18]. In 2011 the Morse/long-range (MLR) potential was fitted to spectroscopic data for the $c(1^3\Sigma_g^+)$ state of Li_2 where there was a gap of $> 5000 \text{ cm}^{-1}$ between data near the bottom of the potential's well, and data at the very top [17]. In 2013 it was found by experiment that vibrational energies predicted from this MLR potential in the very middle of this gap were correct to about 1 cm^{-1} [11]. Therefore, fitting the *ab initio* data to the MLR model can provide reliable energy predictions in regions where *ab initio* points are lacking or are poor in quality.

Therefore, in this paper MLR models that incorporate the long-range theoretical effect of spin-orbit coupling are fitted to the *ab initio* points from [28] for the $2S^{+1}\Pi_{u/g}$ states of Li_2 dissociating to $2S + 3P$. Drawback (3) is not addressed in this paper. However, Born-Oppenheimer breakdown (BOB) corrections could have been added to the *ab initio* points using the molecular electron wavefunction as described in [16]. Alternatively, the entire *ab initio* calculation can be redone using a non-Born-Oppenheimer approach as has been done for up to $6e^-$ [30], but the *a posteriori* approach of doing a Born-Oppenheimer calculation and then adding BOB corrections afterwards has been shown to work better according to the agreement between experiment and theory for BeH [31, 32]. Also, DKH (Douglas-Kroll-Hess) relativistic corrections can be added to the *ab initio* potential as in [33], and QED effects can also be added as was done for H_2 in [34] and HeH^+ in [35]. If any of these answers to drawback (3) were to be addressed by adding corrections to the *ab initio* points of [28], the procedure applied in the present paper for fitting an MLR function to *ab initio* points, could be repeated for even more accurate analytic potentials.

I. EXTENDING THE *AB INITIO* CALCULATIONS

The *ab initio* calculations in [28] did not go beyond 22 \AA . However, beyond a certain length, analytic expressions for the potential can be derived from the theory of atom-atom interactions with disregard for the effect of overlap between each atom's electronic wavefunction. These analytic expressions are based on long-range constants that come from atomic *ab initio* calculations rather than molecular ones, so for Li_2 the calculations only involve $3e^-$ rather than $6e^-$. This means, for example, that a coupled cluster calculation taking account of the full configuration interaction (FCI) of a basis set only needs to go up to triple excitations (CCSDT, whose scaling with respect to the number of basis functions N is $\sim N^8$ and has been implemented since 1987 [36]); whereas a molecular calculation on Li_2 would require all the way up to hexuple excitations (CCSDTQPH, which scales as $\sim N^{14}$, and has been implemented in only very few studies since 2000 [37–42] with basis sets that have not yet gone beyond the cc-pVDZ-DK basis set [42]). Furthermore, $3e^-$ is the limit at which the integrals have been expressed analytically for explicitly correlated Slater wavefunctions, so treating $6e^-$ would either require numerically calculating the integrals (which would be too slow even for small basis sets), or explicitly correlated Gaussian wavefunctions (which do not necessarily have the correct short- and long-range behavior). Therefore, beyond a certain distance the analytic expressions ignoring wavefunction overlap but using long-range constants for Li based on $3e^-$ *ab initio* calculations, are expected to be more accurate than the $6e^-$ *ab initio* calculations of [28] that include wavefunction overlap. The distance at which this trade-off begins to lean in favor of the analytic expressions is heuristically given by the Le Roy radius [43–45].

Another advantage of using the analytic expressions, is that the *ab initio* calculations of [28] do not include the effect of spin-orbit coupling, but for alkali atoms dissociating to $nS + n'P$ asymptotes, the effect of spin-orbit coupling at long-range has been determined analytically [19, 20]. Although all papers discussing these analytic expressions to date only mention $nS + nP$ asymptotes, the expressions are also the same for $nS + n'P$ asymptotes when $n \neq n'$ [21].

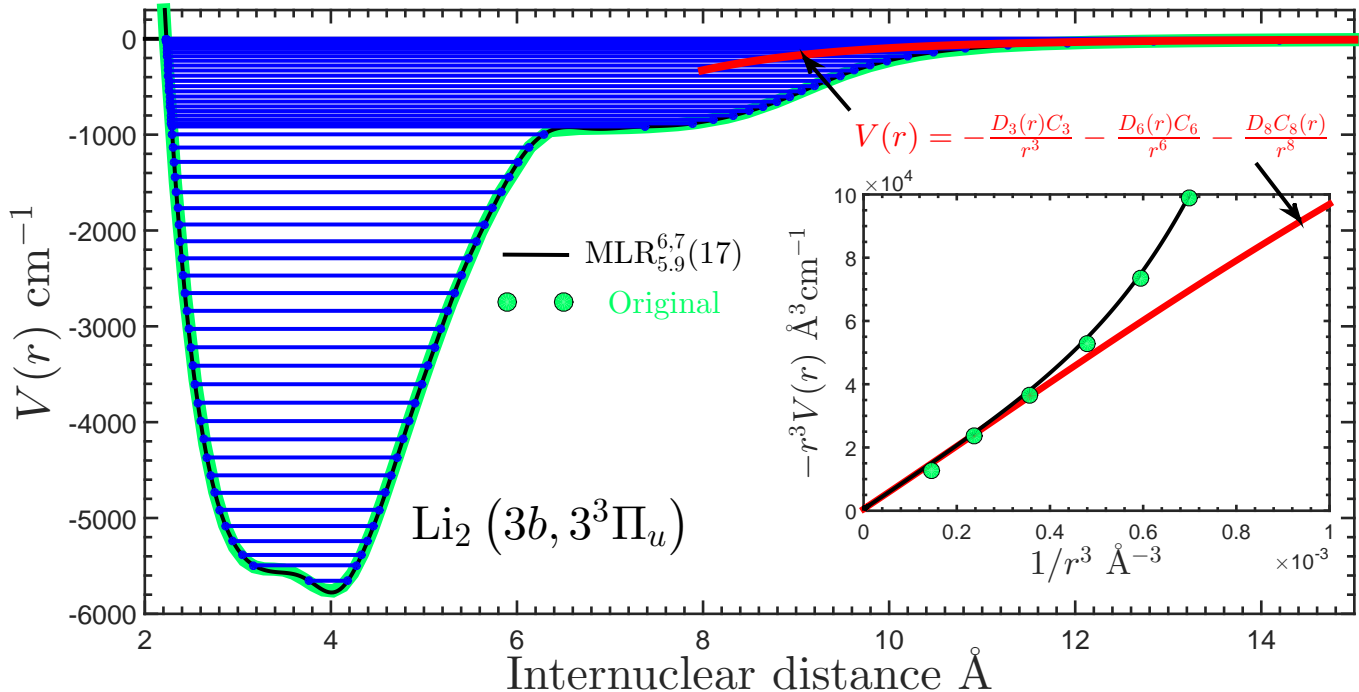
A. Le Roy radii

The m -dependent Le Roy radius is given by Ji *et al.* [45]:

$$R_{\text{LR}-m} \equiv 2\sqrt{3} \left(\langle nlm|z^2|nlm\rangle^{1/2} + \langle n'l'm'|z^2|n'l'm'\rangle^{1/2} \right), \quad (1)$$

where for hydrogen-like atoms we have [45]:

Figure 1. Point-wise original, and analytic MLR potentials for $3b(3^3\Pi_u)$ representing the *ab initio* calculations of [28]. The inset shows the long-range behavior in Le Roy space: it demonstrates that the original *ab initio* points unphysically dip below the theoretical curve, while the MLR behaves correctly.



$$\langle nlm|z^2|nlm\rangle^{1/2} = \left(\frac{1}{3} - \frac{2}{3} \frac{3m^2 - l(l+1)}{(2l+3)(2l-1)} \right)^{1/2} \langle nl|r^2|nl\rangle^{1/2} \quad (2)$$

and for $l = 0$ we have (because m is also 0) [45]:

$$\langle nlm|z^2|nlm\rangle^{1/2} = \frac{1}{\sqrt{3}} \langle r^2 \rangle^{1/2}. \quad (3)$$

This means that if both atoms of a diatomic molecule are in S states, the fact that $l = l' = 0$ reduces Eq. 1 to the original Le Roy radius of [43, 44]:

$$r_{\text{LR}} \equiv 2 \left(\langle r_{\text{A}}^2 \rangle^{1/2} + \langle r_{\text{B}}^2 \rangle^{1/2} \right). \quad (4)$$

However for a hydrogenic atom with $l \neq 0$ we have [45]:

$$\langle nl|r^2|nl\rangle^{1/2} = a_{\mu} \frac{n^2}{Z} \left(1 + \frac{3}{2} \left(1 - \frac{l(l+1) - 1/3}{n^2} \right) \right)^{1/2}, \quad (5)$$

where Z is the effective nuclear charge, $a_{\mu} = a_0 \frac{m_N}{\mu}$ is the Bohr radius scaled by the ratio of the mass of the nucleus m_N to the reduced mass μ of the atom. And for alkali atoms, the principal quantum number n is replaced by $n - \alpha(l)$, where $\alpha(l)$ is the quantum defect and can be found in standard references such as Ref [29] of [45]. Using $\alpha(p) = 1.59$ for Li, assuming that

Table I. m -dependent Le Roy radii for Li_2 electronic states that approach $2s + ml$ in Hartree atomic units and spectroscopic units, and the constituent quantities that are used to calculate these radii.

	$\langle r^2 \rangle$ a.u.	$\langle nlm z^2 nlm\rangle^{1/2}$ a.u.	$r_{\text{LR}-m}(2s+ml)$ a.u.	$r_{\text{LR}-m}(2s+ml)$ Å
2s	17.47 [46]	17.47 [46]	16.7189	8.8473
2p	27.06 [46]	0.3810	27.0	14.0
3p	168.69 [46]	0.5910	40.0	20.1

$\mu_{6\text{Li}} = \frac{m_e M_{6\text{Li}}}{m_e + M_{6\text{Li}}} \approx m_e = 1$ a.u., and using $\langle r^2 \rangle$ values calculated in [46], we are able to calculate Eq. 1 for Li_2 molecules dissociating to various asymptotes, and we present these in Table I.

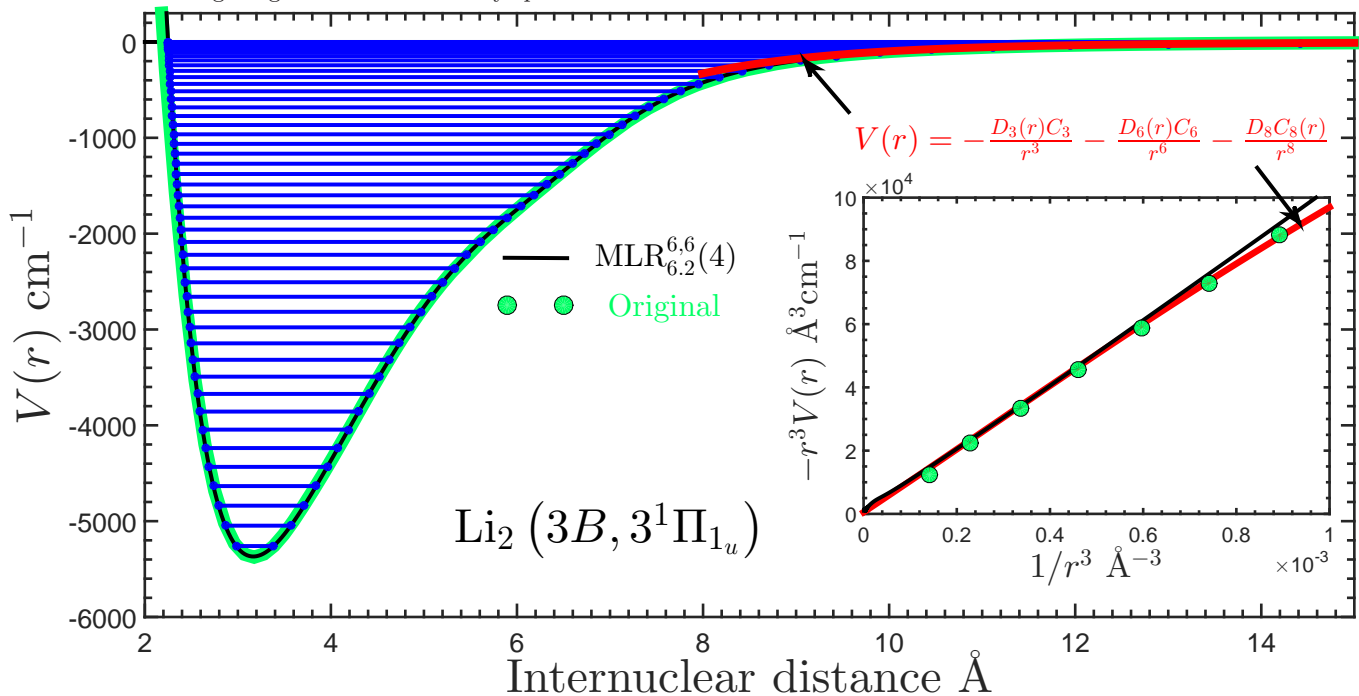
B. Long-range theory

It is well-known that for large internuclear distances, the MLR model becomes, [17]:

$$V(r) \simeq \mathcal{D}_e - u(r) + \dots \quad (6)$$

Therefore, we can define $u(r)$ to be the analytic expression describing the theoretical interaction between the constituent atoms of the molecule. Each $2^S+1\Pi_{u/g}$ state

Figure 2. Point-wise original, and analytic MLR potentials for $3B(3^1\Pi_{1u})$ representing the *ab initio* calculations of [28]. The inset shows the long-range behavior in Le Roy space.



considered in this paper has $\Omega_{u/g}$ daughter states resulting from the spin-orbit coupling that lifts the degeneracy. For the 2_u and 2_g states, which are daughters of $3b(3^3\Pi_g)$ and $3d(3^3\Pi_g)$ respectively, no other $\Omega = 2$ state with

the same u/g symmetry approaches the $2S + 3P$ asymptote, so the potential energy curves at long-range are not strongly influenced by other electronic states. Therefore, these states have the simplest form for $u(r)$:

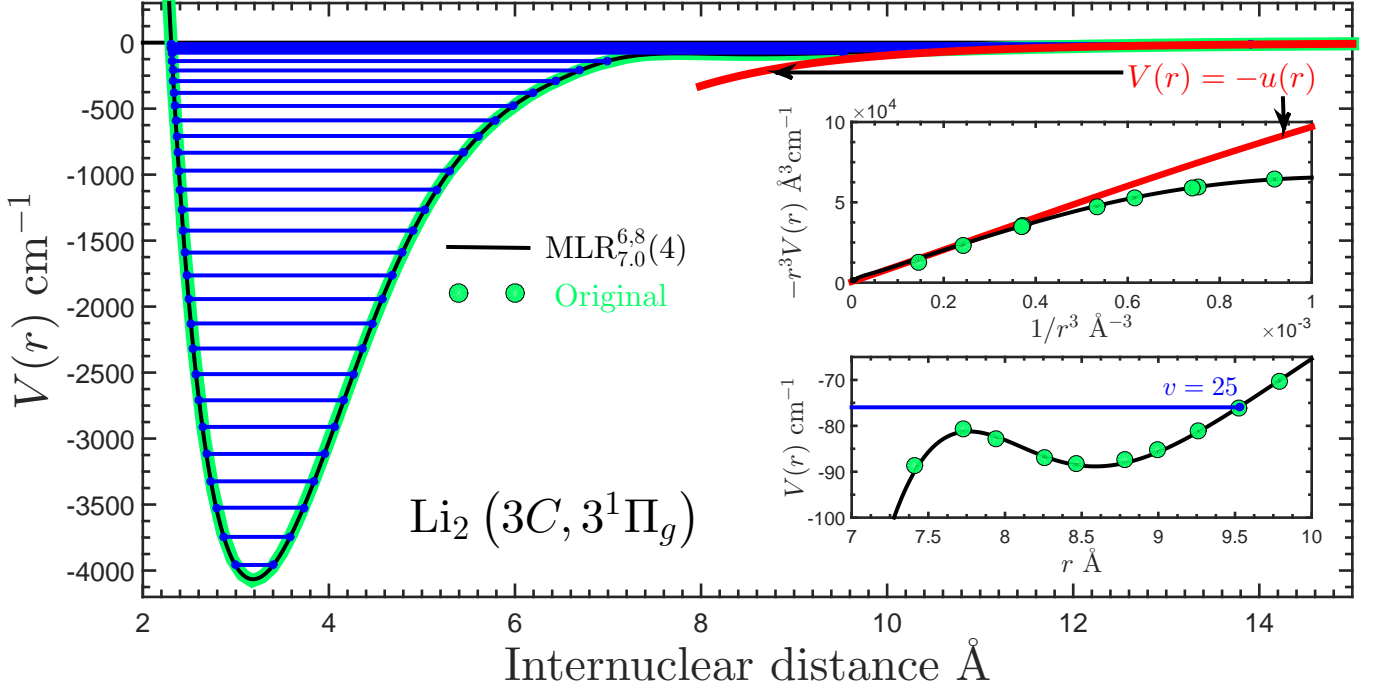
$$u^{2u/g}(r) = - \left(\Delta E - \sum_{m=3,6,8,9,10,11,\dots} \frac{C_m^{(3\Pi_{u/g})}}{r^m} \right) \quad (7)$$

$$= - \left(\Delta E - \frac{C_3^{(3\Pi_{u/g})}}{r^3} - \frac{C_6^{(3\Pi_{u/g})}}{r^6} - \frac{C_8^{(3\Pi_{u/g})}}{r^8} - \frac{C_9^{(3\Pi_{u/g})}}{r^9} - \frac{C_{10}^{(3\Pi_{u/g})}}{r^{10}} - \frac{C_{11}^{(3\Pi_{u/g})}}{r^{11}} \dots \right), \quad (8)$$

where the zero of energy is the $\text{Li}(2S_{1/2}) + \text{Li}(3P_{1/2})$ asymptote, and $\Delta E \equiv \Delta E_{3^2P_{3/2} \leftarrow 3^2P_{1/2}}$ is included since the 2_u and 2_g states both dissociate to $\text{Li}(2S_{1/2}) + \text{Li}(3P_{3/2})$. The $3b(3^3\Pi_u)$ state additionally has a daughter state of 1_u symmetry, along with $3B(3^1\Pi_u)$; and the $3d(3^3\Pi_g)$ state additionally has a daughter state of 1_g symmetry, along with $3C(3^1\Pi_g)$. Since all $1_{u/g}$ states approaching $2S + 3P$ have two other $1_{u/g}$ states of the same u/g symmetry approaching $2S + 3P$, the $u(r)$ for these states is defined as the highest, middle, or lowest energy eigenvalue of the following 3×3 matrix (including the prefactor of -1) depending on whether the state in question is the lowest, middle, or highest in energy respectively:

$$\mathbf{u}^{1u/g}(r) = \quad (9)$$

Figure 3. Point-wise original, and analytic MLR potentials for $3C(3^1\Pi_g)$ representing the *ab initio* calculations of [28]. The top inset shows the long-range behavior in Le Roy space, and the bottom inset shows that the MLR successfully captures the tiny second minimum which has a depth of $\approx 8.5 \text{ cm}^{-1}$.



$$- \left(\begin{array}{ccc} \frac{1}{3} \sum_m \frac{C_m^{(3/1\Sigma^+_{u/g})} + C_m^{(1/3\Pi_{u/g})} + C_m^{(3/1\Pi_{u/g})}}{r^m} & \frac{1}{3\sqrt{2}} \sum_m \frac{-2C_m^{(3/1\Sigma^+_{u/g})} + C_m^{(1/3\Pi_{u/g})} + C_m^{(3/1\Pi_{u/g})}}{r^m} & \frac{1}{\sqrt{6}} \sum_m \frac{-C_m^{(1/3\Pi_{u/g})} + C_m^{(3/1\Pi_{u/g})}}{r^m} \\ \frac{1}{3\sqrt{2}} \sum_m \frac{-2C_m^{(3/1\Sigma^+_{u/g})} + C_m^{(1/3\Pi_{u/g})} + C_m^{(3/1\Pi_{u/g})}}{r^m} & \Delta E + \frac{1}{6} \sum_m \frac{4C_m^{(3/1\Sigma^+_{u/g})} + C_m^{(1/3\Pi_{u/g})} + C_m^{(3/1\Pi_{u/g})}}{r^m} & \frac{1}{2\sqrt{3}} \sum_m \frac{-C_m^{(1/3\Pi_{u/g})} + C_m^{(3/1\Pi_{u/g})}}{r^m} \\ \frac{1}{\sqrt{6}} \sum_m \frac{-C_m^{(1/3\Pi_{u/g})} + C_m^{(3/1\Pi_{u/g})}}{r^m} & \frac{1}{2\sqrt{3}} \sum_m \frac{-C_m^{(1/3\Pi_{u/g})} + C_m^{(3/1\Pi_{u/g})}}{r^m} & -\Delta E + \frac{1}{2} \sum_m \frac{C_m^{(1/3\Pi_{u/g})} + C_m^{(3/1\Pi_{u/g})}}{r^m} \end{array} \right) \quad (10)$$

The notation $^{1/3}\Lambda_{u/g}$ means ($^1\Lambda_u$ or $^3\Lambda_g$). The zero of energy is once again the $\text{Li}(2S_{1/2}) + \text{Li}(3P_{1/2})$ asymptote. Finally, the $3b$ state additionally has 0_u^+ and 0_u^- daughter states, and the $3d$ state additionally has 0_g^+ and 0_g^- daughter states. Since all $0_{u/g}^{+/-}$ states approaching $2S + 3P$ have one other $0_{u/g}^{+/-}$ state of the same u/g symmetry and the same $+/-$ symmetry approaching $2S + 3P$, the $u(r)$ for these states is defined as the higher, or lower energy eigenvalue of the following 2×2 matrix (including the prefactor of -1) depending on whether the state in question is lower, or higher in energy respectively:

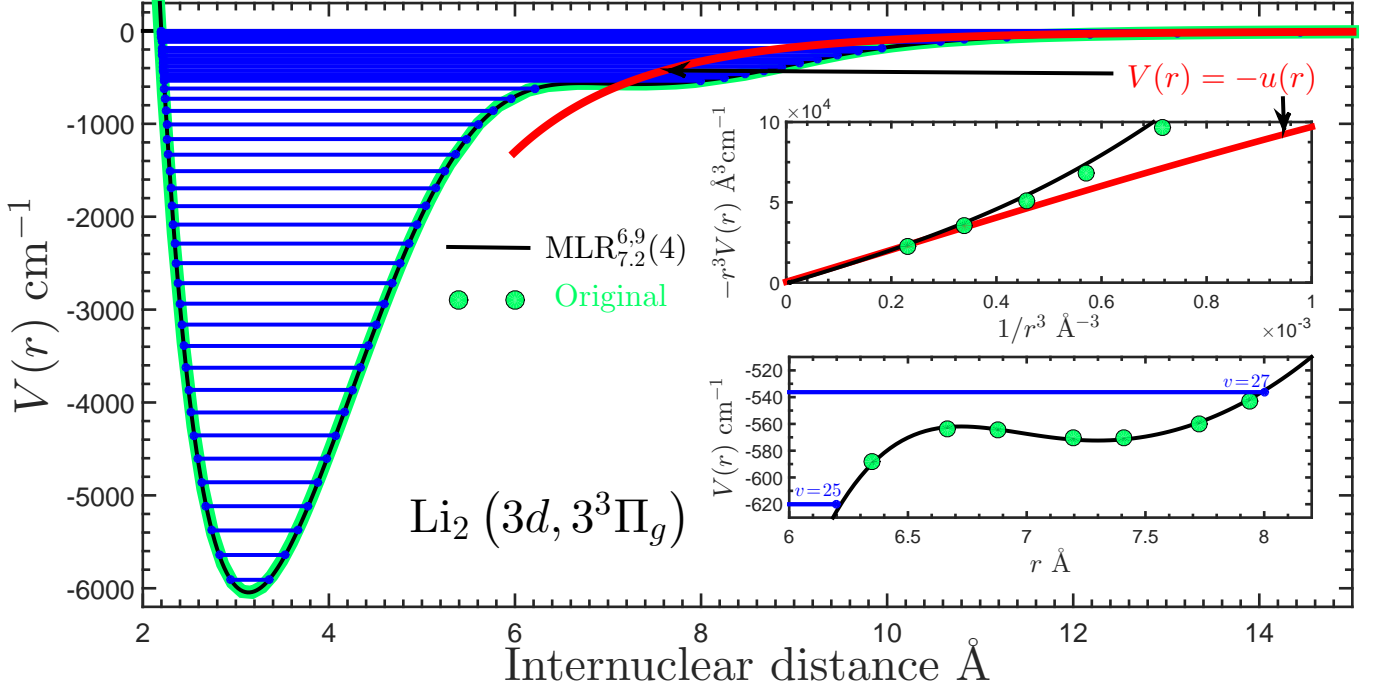
$$\mathbf{u}_{u/g}^{0+/-}(r) = - \left(\begin{array}{cc} \frac{1}{3} \sum_{m=3,6,8,9,10,11,\dots} \frac{C_m^{(3/1\Sigma^+_{u/g})} + 2C_m^{(1/3\Pi_{u/g})}}{r^m} & \frac{\sqrt{2}}{3} \sum_{m=3,6,8,9,10,11,\dots} \frac{C_m^{(3/1\Sigma^+_{u/g})} - C_m^{(1/3\Pi_{u/g})}}{r^3} \\ \frac{\sqrt{2}}{3} \sum_{m=3,6,8,9,10,11,\dots} \frac{C_m^{(3/1\Sigma^+_{u/g})} - C_m^{(1/3\Pi_{u/g})}}{r^m} & -\Delta E + \frac{2}{3} \sum_{m=3,6,8,9,10,11,\dots} \frac{C_m^{(3/1\Sigma^+_{u/g})} + C_m^{(1/3\Pi_{u/g})}}{r^m} \end{array} \right) \quad (11)$$

The zero of energy is once again the $\text{Li}(2S_{1/2}) + \text{Li}(3P_{1/2})$ asymptote.

Since the leading term not shown in Eq. 6 is $\frac{u(r)^2}{4\mathcal{D}_e}$, the contribution of the C_3 terms to the long-range form of the potential, will interfere with the desired C_6 and

C_8 terms, and all C_9 and C_{11} terms will therefore have spurious contributions from the cross-terms formed by the products of the C_3 terms with the C_6 and C_8 terms

Figure 4. Point-wise original, and analytic MLR potentials for $3d(3^3\Pi_g)$ representing the *ab initio* calculations of [28]. The top inset shows the long-range behavior in Le Roy space, and the bottom inset shows that the MLR successfully captures the tiny second minimum which has a depth of $\approx 13.5 \text{ cm}^{-1}$.



respectively. We fix this in the same way as was done for C_6 and C_9 in [11, 12, 16–18, 47], by applying a transformation to all C_6 , C_9 , and this time also C_{11} terms:

$$C_6 \rightarrow C_6 + \frac{C_3^2}{4\mathcal{D}_e} \quad (12)$$

$$C_9 \rightarrow C_9 + \frac{C_3 C_6}{2\mathcal{D}_e}, \quad (13)$$

$$C_{11} \rightarrow C_{11} + \frac{C_3 C_8}{2\mathcal{D}_e}. \quad (14)$$

where the transformation in Eq. 12 has to be made first due to Eq. 13's dependence on C_6 .

Additionally, the long-range formulas in terms of C_m constants in Eqs. 8,10,11 were derived under the assumption that two free atoms are interacting with each other, and there is no overlap of the electrons' wavefunctions as would be in a bound molecule. To take into account the effect of electron overlap, we use the damping function form from [48]:

$$C_m \rightarrow C_m D_m^{(s)}(r) \quad (15)$$

$$D_m^{(s)}(r) \equiv \left(1 - e^{-\left(\frac{b^{(s)} \rho r}{m} + \frac{c^{(s)} (\rho r)^2}{\sqrt{m}} \right)} \right)^{m+s}, \quad (16)$$

where for interacting atoms A and B, $\rho \equiv \rho_{AB} = \frac{2\rho_A \rho_B}{\rho_A \rho_B}$, in which $\rho_X \equiv (I^X/I^H)^{2/3}$ is defined in terms of the ionization potentials of atom X, denoted (I^X) , and hydrogen

(I^H). We use $s = -1$, which as shown in [48], means that the MLR potential has the physically desired behavior $V(r) \simeq 1/r^2$ in the limit as $r \rightarrow 0$. For $s = -1$, the system independent parameters take the values $b^{(-1)} = 3.30$, and $c^{(-1)} = 0.423$ [48].

C. Long-range constants

For electronic states of Li_2 approaching the $2S + 2P$ asymptote, the $C_{3,6,8}$ constants for all electronic state symmetries have been calculated with finite-mass corrections for ^6Li and ^7Li [49], and even an attempt at relativistic corrections has been made for the C_3 constants [50, 51]. Furthermore, for $2S + 2P$, third-order perturbation theory has been used to calculate non-relativistic infinite-mass values for C_9 and C_{11} [13], meaning that it was possible to also include the non-relativistic infinite-mass value of C_{10} calculated in [46].

The situation is much less convenient for $2S + 3P$. No third-order perturbation theory calculation has been done for C_9 or C_{11} , and without C_9 it does not make sense to include the C_{10} value, which was calculated in the same study as for the $2S + 2P$ asymptote [46]. Also, no finite-mass or relativistic corrections have been calculated for the $C_{3,6,8}$ values associated with $2S + 3P$. Nevertheless, we have available the non-relativistic infinite-mass values for $C_{3,6,8}$ that were calculated in [46], and these were reported with an order of magnitude higher precision than in the very highly cited 1995 paper of

Table II. The best currently available long-range constants for Li_2 electronic states that dissociate to $2S + 3P$ (in Hartree atomic units). All values come from [46] and were calculated without relativistic corrections, and under the assumption that both Li nuclei have infinite mass.

	$^{1/3}\Sigma_{u/g}$	$^{3/1}\Sigma_{u/g}$	$^{1/3}\Pi_{u/g}$	$^{3/1}\Pi_{u/g}$
C_3	0.0033314	-0.0033314	-0.0016657	0.0016657
C_6	3.8236×10^4	3.8236×10^4	2.0282×10^4	2.0282×10^4
C_8	2.4870×10^7	2.3183×10^7	7.8976×10^5	3.7222×10^5

Marinescu and Dalgarno [52], and only one order of magnitude lower precision than the $2S + 2P$ values which are known (see Table 2 in [16] for a list of the best known C_m constants for each symmetry approaching $2S + 2P$). All C_m constants that are used in this study for $2S + 3P$ are given in Table II.

II. MLR POTENTIALS

It has been suggested that fully analytic potentials [53], and specifically the MLR [54] may not have the flexibility required to capture some features such as multiple minima and shelves (see examples of these features appearing in $2S - 3P$ potentials of Li_2 in Figs 1-4). While no attempt (as far as I am aware) has thus far been made to use a fully analytic potential to capture such features, an increasing number of applications of the MLR potential after the publications of [53, 54] has made it a strong case for a “universal” potential form. MLR-type potentials have successfully described spectroscopic data for many electronic states of many diatomic molecules [11, 12, 16–18, 31, 48, 55–72]. It has also become customary to fit *ab initio* data for diatomic [73–79] and polyatomic [66, 80–84] systems to MLR models. Therefore, we use the MLR model in this study, and the results here support the idea of the MLR model being a strong candidate for a “universal” model for potential energy curves and surfaces.

All MLR potentials were made by fitting to the *ab initio* points of Ref. [28] with the program DPotFIT [85]. Since this is a non-linear least-squares fitting, ‘starting parameters’ are needed in order to allow DPotFit to achieve reasonable fits. Starting parameters were obtained from the program BetaFIT [85]. When fitting to *ab initio* points, DPotFIT aims to minimize the dimensionless root mean square deviation:

$$dd \equiv \sqrt{\frac{1}{N_{\text{data}}} \sum_{i=1}^{N_{\text{data}}} \left(\frac{V_{\text{MLR}}(i) - V_{ab \text{ initio}}(i)}{u_{ab \text{ initio}}(i)} \right)^2}, \quad (17)$$

where $V_{\text{MLR}}(i)$ and $V_{ab \text{ initio}}(i)$ are the values of the respective potentials at the i^{th} internuclear distance value (the order of course does not matter) and N_{data} is the

total number of *ab initio* points to which the MLR potential is being fitted. $u_{ab \text{ initio}}(i)$ is the uncertainty in the i^{th} *ab initio* point, so that the MLR potential is likely to lie more closely to *ab initio* points at distances where the *ab initio* calculation is expected to be more reliable, and the requirement for the MLR potential to match the *ab initio* is less harsh in areas where the *ab initio* calculation is expected to be less accurate.

It is extremely hard to determine accurate estimates on the uncertainties for *ab initio* points. The *ab initio* points we are using from [28] were all calculated with the same basis set (which the authors denoted by ANO-RCC+), therefore there is no indication of the size of the basis set error. Furthermore, all of their calculations were done with the same number of excitations included in their coupled cluster method: FS-CCSD(2,0) only includes 1- and 2-electron excitations, so it would be extremely unlikely to estimate the deviation from the full 6-electron (FCI) limit. Perhaps even more importantly, the calculations of [28] neglected relativistic, spin-orbit, and non-Born-Oppenheimer effects, so accurately estimating $u_{ab \text{ initio}}(i)$ might seem impossible.

However, in my recent benchmark paper [16], it was shown that none of the vibrational energies associated with the *ab initio* potential from [28] for the $b(1^3\Pi_u)$ state of Li_2 , deviated from the empirical potential’s vibrational energies by more than 12 cm^{-1} . Since that *ab initio* potential used the same basis set and method as their potentials for the electronic states approaching $2S + 3P$, I aimed to make $V_{\text{MLR}}(i) - V_{ab \text{ initio}}(i)$ less than 15 cm^{-1} for all i except at very small internuclear distances near the $r = 0$ singularity where the inner wall of the potential rapidly increases, crosses the dissociation limit, and then attains extremely large energy values. The exact values used for $u_{ab \text{ initio}}(i)$ that were used are presented in Tables IV, VI, VIII and X. Furthermore, there are places in which it was desirable to make $u_{ab \text{ initio}}(i)$ smaller than 15 cm^{-1} . This was in places where the potentials from [28] had features such as tiny second minima, tiny shelves, or any other type of abrupt change. The subsections (below) for each electronic state will describe in detail the nature of these features and how this affected the choice of $u_{ab \text{ initio}}(i)$ (once again the exact values are given in Tables IV, VI, VIII and X).

The MLR model was fitted to the points from [28] with various manually adjusted values of the MLR parameters ($N_\beta, p, q, r_{\text{ref}}$) in search for the lowest dd according to Eq. 17 such that increasing N_β no longer reduced dd significantly further than the best dd obtained with the previous increase in N_β . Details for each electronic state are described in the subsections below which focus on each state.

A. The $3b(3^3\Pi_u)$ state

The first b state of Li_2 dissociates to the $2S + 2P$ asymptote. A very detailed analysis of theory vs exper-

Table III. Parameters defining the $\text{MLR}_{p,q}^{r_{\text{ref}}}(N_\beta)$ potentials fitted to *ab initio* points from [28], and with long-range functions $u(r)$ defined according to the descriptions in section I C, and with long-range constants presented in Table II. Numbers in parentheses are 95% confidence limit uncertainties in the last digit(s) shown, calculated from the least-squares fitting procedure.

$3b(3^3\Pi_u)$ MLR $_{6,7}^{5,9}(17)$				$3B(3^1\Pi_u)$ MLR $_{6,6}^{6,2}(4)$				$3C(3^1\Pi_g)$ MLR $_{6,8}^{7,0}(8)$				$3d(3^3\Pi_g)$ MLR $_{6,3}^{7,2}(4)$			
\mathfrak{D}_e	5765.593	cm^{-1}		\mathfrak{D}_e	5368.8(38)	cm^{-1}		\mathfrak{D}_e	4066.0467	cm^{-1}		\mathfrak{D}_e	6045.135	cm^{-1}	
r_e	3.984	527(23)	\AA	r_e	3.165	8(18)	\AA	r_e	3.184	402(23)	\AA	r_e	3.137	142(23)	\AA
β_0	0.378369938	β_{10}	-3213.8074	β_0	-0.8509	β_{10}	0.78516117	β_0	0.78516117	β_{10}	0.78516117	β_0	0.78516117	β_{10}	0.78516117
β_1	0.918196351	β_{11}	1673.5923	β_1	-0.592	β_{11}	2.3951022	β_1	2.3951022	β_{11}	2.39510218	β_1	2.39510218	β_{11}	2.39510218
β_2	2.08782371	β_{12}	6482.429	β_2	-0.038	β_{12}	6.950787	β_2	6.950787	β_{12}	6.9507868	β_2	6.9507868	β_{12}	6.9507868
β_3	0.96103485	β_{13}	-1705.759	β_3	0.74	β_{13}	-4.68625	β_3	-4.68625	β_{13}	-4.686246	β_3	-4.686246	β_{13}	-4.686246
β_4	-46.0405588	β_{14}	-7329.75	β_4	0.57	β_{14}	-5.17796	β_4	-5.17796	β_{14}	-5.17796	β_4	-5.17796	β_{14}	-5.17796
β_5	-117.75187	β_{15}	822.19			β_{15}	5.22029	β_5	5.22029	β_{15}	5.22029	β_5	5.22029	β_{15}	5.22029
β_6	271.27645	β_{16}	4297.08			β_{16}	7.5253	β_6	7.5253	β_{16}	7.5253	β_6	7.5253	β_{16}	7.5253
β_7	880.09337	β_{17}	-122.54			β_{17}	-2.100	β_7	-2.100	β_{17}	-2.100	β_7	-2.100	β_{17}	-2.100

iment for the first b state of Li_2 was recently reported [16], which summarized 14 different experiments providing new information on the $b(1^3\Pi_u)$ state since 1983 [1, 86–98], and mentioned several other papers that involved this state without providing information on any new levels. Due to the spin-orbit coupling between b states of alkali dimers and their respective $A(1^1\Sigma_u^+)$ states, recent experimental and theoretical papers have studied the lowest b state of Rb_2 , [57, 99, 100], NaCs [101], KCs [102], RbCs [103], Cs_2 [104] and NaK [105].

It is thus surprising that no experiments have been reported for the second b state of Li_2 , which dissociates to the $2P + 2P$ asymptote. The present paper is concerned with the third b state, which dissociates to $2S + 3P$. The *ab initio* potential for $3b(3^3\Pi_u)$ from [28] has a small shelf-like feature before the minimum, and another much longer one closer to dissociation (see Fig. 1). The first shelf is located between $v = 0$ and $v = 1$, and it lasts from about $3.2 - 3.6 \text{ \AA}$. The second shelf starts after $v = 27$ and lasts from about $6.4 - 8 \text{ \AA}$. Despite these fairly pronounced shelf features, at the resolution of the *ab initio* points (which is about 0.1 \AA), the $3b$ state only has one minimum!

In Section II it was mentioned that, with the exception of points at very small values of r , the goal was to match all *ab initio* points of [28] to within $\pm 15 \text{ cm}^{-1}$ (and points at larger values of r even better), since this was about the level of accuracy found when comparing *ab initio* points [28] to an empirical potential for $b(1^3\Pi_u)$ in [16]. Preliminary fits used such a weighting scheme for the least-squares fitting, except with points comprising the two shelves mentioned in the previous paragraph, weighted with much smaller uncertainties. This was especially important for the second shelf, which only spanned a range of $< 100 \text{ cm}^{-1}$: Because if the discrepancy between the MLR and *ab initio* was -15 cm^{-1} at one point, and $+15 \text{ cm}^{-1}$ at another point, the 30 cm^{-1} range of discrepancy would constitute a significant portion of the range of the entire shelf itself. After these

preliminary fits, it was found that in order to get the MLR matching the original data with the desired precision, it helped to decrease the uncertainties on the non-shelf *ab initio* points to slightly below $\pm 15 \text{ cm}^{-1}$. The best fits were found with the weights shown in Table IV. Once these final weights were chosen, fits were performed for 252 different combinations of the MLR parameters $(N_\beta, p, q, r_{\text{ref}})$, with $4 \leq N_\beta \leq 17$, $6 \leq p \leq 8$, $2 \leq q \leq 8$, ($5 \leq r_{\text{ref}} \leq 6.5$) \AA , though not every point in the convex hull formed by these ranges was used. For example, some fits were done with $(p, q) = (6, 2)$ and some fits were done with $(p, q) = (8, 6)$ but it did not seem necessary to do fits with $(p, q) = (8, 2)$. The best fit was found with $(N_\beta, p, q, r_{\text{ref}}) = (17, 6, 7, 5.9 \text{ \AA})$, and had $dd = 1.548$, while the best fit with $N_\beta = 16$ was with $(N_\beta, p, q, r_{\text{ref}}) = (16, 6, 6, 5.3 \text{ \AA})$ and had $dd = 2.790$. Apart from in the inner wall of the potential, the worst discrepancy between the MLR and the original points for this $N_\beta = 16$ case it was $> 30 \text{ cm}^{-1}$, while for this $N_\beta = 17$ case was $< 11 \text{ cm}^{-1}$ so it was quite easy to select the $N_\beta = 17$ fit. Since this $N_\beta = 17$ fit satisfied all of our desiderata, $N_\beta = 18$ fits were not explored.

The final MLR parameters for the chosen case are given in Table III. The inset of Fig. 1 shows the long-range behavior of the MLR potential and the original *ab initio* points of [28] in Le Roy space, and compares them to the theoretical long-range potential based on Eq. 8 and the long-range constants in Table II. The agreement is surprisingly excellent, however after about 17.7 \AA ($1/r^3 \approx 0.0018 \text{ \AA}^{-3}$) we see that the original points dip below the theoretical curve, which should not happen because C_8 is attractive (see Section 4.3 of [56], for example). The fact that the MLR potential matches the theoretical curve in this regard, is yet another advantage of using an MLR to represent the *ab initio* points. Furthermore, while not shown in Fig. 1, the theoretical long-range curve *without* damping, matches the damped curve shown in the figure to graphical accuracy at least in the range $14 \text{ \AA} \leq r \leq \infty$ ($0 \leq 1/r^3 = 0.00036 \text{ \AA}^{-3}$), so

this conclusion about the original points spuriously dipping below the theoretical curve is true whether or not long-range damping is considered.

B. The $3B(3^1\Pi_u)$ state

The first B state has a barrier before dissociating to the $2S + 2P$ asymptote, and has therefore been the subject of many empirical studies [53, 106–111]. It has also been used to study other states, such as in [94, 112–115]. The second B state potential (sometimes called the “ $C^1\Pi_u$ state” rather than the $2B$ state) dissociates to $2P + 2P$ and hugs the inside of the first minimum of the $2A(1^1\Sigma_u^+)$ potential, and due to the perturbations between these $2B$ and $2A$ states, there have been many empirical studies of the $2B$ state [96, 115–119].

The present paper is concerned with third B state. The $3B$ state dissociates to $2S + 3P$ and there has only been one experiment which studied the third B state (sometimes called the “ $D^1\Pi_u$ state”) [116], which was over 55 years ago! The authors of that work mentioned in their paper that they were not able to confidently assign vibrational quantum numbers to their data, and therefore they were only able to conclude that $T_e < 34140 \text{ cm}^{-1}$ and $\omega_e \approx 250 \text{ cm}^{-1}$. In that study, the anharmonic values $x_e\omega_e$, equilibrium rotational constants B_e , and dissociation energies \mathfrak{D}_e were determined for the $2B$ state of Li_2 and for the $2B$ and $3B$ states of Na_2 , but not for the $3B$ state of Li_2 .

It is no surprise that none of the experiments on the $2B$ state showed any indication of a barrier in the potential, because the leading long-range term (C_5) is attractive [46]. However, it is perhaps surprising that the *ab initio* potential of [28] for the $3B$ state does not have a barrier (at least before the calculations stopped at about 21 Å), because the leading long-range interaction term (C_3) for this state is repulsive [46]. There is however a good theoretical explanation for the lack of barrier in the $3B$ state. The long-range potential for $3B$ is not just a simple sum of inverse powers ($-C_3/r^3 - C_6/r^6 \dots$), but it is the middle eigenvalue of the 3×3 spin-orbit interaction matrix of Eq. 10, which involves the $6a(6^3\Sigma_u)$ and $3b(3^3\Pi_u)$ states. For large internuclear distances, the $6a$ state pushes down on the $3B$ state enough to remove the barrier. Indeed, numerical calculations of the eigenvalues of the 3×3 matrix show that the potential is attractive at all distances (beyond the repulsive inner wall for $r \ll r_e$). This 3×3 matrix for $3B$ is the exact same as the one for the first B state, which *does* have a barrier, but for the $3B$ state the C_3 is three orders of magnitude smaller than for the first B state, and the C_6 is one order of magnitude bigger than for the first B state [46]. This highlights the importance of using the 3×3 coupling matrix because a simple inverse power sum with a negative leading long-range term (such as the negative C_3 in the present case) is guaranteed to have a barrier, and there was even a barrier when using the middle eigenvalue of

the 3×3 coupling matrix for the $2S + 2P$ values of C_m , but the specific values of C_m at $2S + 3P$ seem to be past a bifurcation point at which the barrier is lost.

Since alkali parent states of $B(1^1\Pi_u)$ symmetry only have one spin-orbit daughter state ($\Omega_{u/g} = 1_u$), we do not need to worry about defining the MLR long-range function $u(r)$ in a piece-wise manner, and it is simply defined as the middle eigenvalue of the 3×3 interaction matrix of Eq. 10. Also, since there are no features such as barriers, multiple minima or shelves, the weighting strategy was straightforward. Preliminary fits were done with all points from [28] being weighted with uncertainty $\pm 15 \text{ cm}^{-1}$ if $V(r) < -100 \text{ cm}^{-1}$, with $\pm 5 \text{ cm}^{-1}$ if $V(r) < -20 \text{ cm}^{-1}$, with $\pm 1 \text{ cm}^{-1}$ if $V(r) < 1 \text{ cm}^{-1}$ and $\pm 0.5 \text{ cm}^{-1}$ for the one point for which $-1 \text{ cm}^{-1} < V(r) < 0 \text{ cm}^{-1}$. It was then found that most uncertainties could be even further reduced without making the fitting too difficult, and that for very small values of r it was very difficult to achieve $\pm 15 \text{ cm}^{-1}$ agreement in the fit. In the end, the points from [28] for the smallest values of r (with $V(r) > -4000 \text{ cm}^{-1}$) were weighted with uncertainty $\pm 100 \text{ cm}^{-1}$, and all other points were weighted with $\pm 1 \text{ cm}^{-1}$, except for the last point which was weighted with $\pm 0.5 \text{ cm}^{-1}$ because $V(r)$ itself was only $\approx -0.7 \text{ cm}^{-1}$. These final weights are shown in Table VI.

Once these final weights were chosen, fits were performed for 150 different combinations of the MLR parameters ($N_\beta, p, q, r_{\text{ref}}$), with $3 \leq N_\beta \leq 5$, $6 \leq p \leq 7$, $2 \leq q \leq 7$, ($5 \leq r_{\text{ref}} \leq 10$) Å, though not every point in the convex hull formed by these ranges was used. The best fit with $N_\beta = 4$ was with $(p, q, r_{\text{ref}}) = (6, 6, 6.2 \text{ Å})$ which had $dd = 4.307$ while the best fit found using $N_\beta = 5$ was only marginally better ($dd = 4.128$) and no fits were found with $N_\beta = 3$ that had $dd < 10$. Therefore, the choice of MLR model for this electronic state was easy to make, and the final parameters are listed in Table III.

C. The $3C(3^1\Pi_g)$ state

The first $C(1^1\Pi_g)$ state dissociates to $2S + 2P$ and was not studied in detail until 1990 [120]. This was 11 years after the second state of $C(1^1\Pi_g)$ symmetry (sometimes called the “ $G^1\Pi_g$ state” since it was given this name in [121]) was studied in detail in 1979 [122]. This $2C$ state dissociates to $2P + 2P$ and was studied again in a series of follow-up papers by Bernheim *et al.* [4, 121, 123]. Impressively, empirical spectroscopic constants have also been reported for all Rydberg states in the series $nd\pi^1\Pi_g$ for $n = 3 - 15$ (!) [4, 123]. In the same paper, it was determined that the $n = 3$ state in this series is in fact the $2C$ state.

The third C state is the subject of the present work, since it dissociates to $2S + 3P$. It only has one spin-orbit daughter state, which has 1_g symmetry and couples to the 1_g daughters of the $3c(3^3\Sigma_g^+)$ and $3d(3^3\Pi_g)$

states. The potential energy of the $3C$ state's 1_g daughter is given by the middle eigenvalue of the appropriate 3×3 matrix. Preliminary fits were done with the same weighting scheme as for the $3B$ state, except with the points surrounding the second minimum weighted more strongly (with $\pm 0.5 \text{ cm}^{-1}$), since the depth of this well is $< 10 \text{ cm}^{-1}$ and therefore it would not be satisfactory to fit to these points with an agreement of only $\pm 15 \text{ cm}^{-1}$! It was then found that many points could be weighted more strongly without making the fitting too difficult. The weights were adjusted to $\pm 10 \text{ cm}^{-1}$ for points at the smallest values of r ($V(r) > -3000 \text{ cm}^{-1}$), to $\pm 5 \text{ cm}^{-1}$ for the rest of the points with $V(r) < -1000 \text{ cm}^{-1}$, to $\pm 1 \text{ cm}^{-1}$ for points with $V(r) < -1 \text{ cm}^{-1}$, except for the points near the second minimum, and the very last point for which $V(r) \approx -0.75 \text{ cm}^{-1}$. The final weights are presented in Table VIII.

With these final weights, fits were performed for 302 different combinations of the MLR parameters $(N_\beta, p, q, r_{\text{ref}})$, with $2 \leq N_\beta \leq 11$, $6 \leq p \leq 11$, ($4 \leq r_{\text{ref}} \leq 12$) Å, though not every point in the convex hull formed by these ranges was used. The best fit with $N_\beta = 8$ was with $(p, q, r_{\text{ref}}) = (6, 5, 7.5 \text{ Å})$ which had $dd = 1.612$, but this potential did not capture the second minimum very well (particularly, it approaches the barrier leading to that minimum with the *ab initio* point of $V(7.408 \text{ Å}) = -88.76 \text{ cm}^{-1}$ being represented with a discrepancy of $> 5.5 \text{ cm}^{-1}$). The best fit with $N_\beta = 8$ which captured $V(7.408 \text{ Å})$ with a discrepancy of $< 2 \text{ cm}^{-1}$ was with $(p, q, r_{\text{ref}}) = (6, 8, 7.0 \text{ Å})$ which had $dd = 3.536$. None of the $N_\beta = 7$ models that reproduced $V(7.408 \text{ Å})$ with discrepancy $< 2 \text{ cm}^{-1}$ had an overall $dd < 4$, and while $N_\beta = 9$ fits were found with discrepancies for this point $< 2 \text{ cm}^{-1}$ and overall dd as low as 2.593, there were no points beyond $r = 2.6 \text{ Å}$ for which the $N_\beta = 8$ case with $dd = 3.536$ misrepresented an original point by $> 18 \text{ cm}^{-1}$ (the highest discrepancy was 17.37 cm^{-1} at 3.175 Å , and among these $N_\beta = 9$ cases, the lowest discrepancy for this same point was 12.70 cm^{-1}). While deciding not to go beyond $N_\beta = 8$ was not an easy choice, there is not much reason to believe that the calculation in [28] for $V(3.175 \text{ Å})$ is so precise that representing it more closely by $\approx 5 \text{ cm}^{-1}$ is worth adding an extra parameter. Here it is mentioned that while the comparison against the empirical potential in [16] for the lowest b state showed no discrepancy of $> 12 \text{ cm}^{-1}$, that paper also noted the surprisingly small effect of Born-Oppenheimer breakdown in that system, meaning that it is likely that the potentials in [28] for other electronic states (especially ones approaching $2S - 3P$, which seem to interact with each other more than the ones approaching the $2S - 2P$ state) will be accurate to slightly less precision than $\pm 12 \text{ cm}^{-1}$. The final MLR parameters for the chosen model are listed in Table III.

D. The $3d(3^3\Pi_g)$ state

The first d state has a potential energy curve which approaches the $2S + 2P$ asymptote, but the *ab initio* calculations of [28] indicate that it has no bound states. Therefore, it is no surprise that no bound levels have been found in experiments on this state, though it was indeed involved in some experiments [124–126]. While the prediction in [28] that the first d state has no bound levels is likely to be true, it should be noted that *ab initio* predictions of this sort are not always reliable. The 1995 *ab initio* study of [26] predicted that the $1^1\Sigma_u^-$ state would have no bound levels, but the 2014 calculations of [28] found there to be a dissociation energy of $\mathfrak{D}_e = 14 \text{ cm}^{-1}$ and an equilibrium harmonic frequency of $\omega_e = 10 \text{ cm}^{-1}$, indicating the existence of at least two bound vibrational levels! Likewise, the 2006 *ab initio* study of [27] found the $1^3\Delta_u$ state to not have any bound levels, but the earlier 1995 study of [26] and the 2014 study of [28] both predicted $\mathfrak{D}_e \geq 3430 \text{ cm}^{-1}$ and $\omega_e \leq 255 \text{ cm}^{-1}$.

The second d state has been studied extensively. Spectroscopic measurements for $2d$ were made in [1, 3, 6–8, 96, 97], and $2d$ was also used in various other experimental studies such as [91, 92, 94, 125–129].

The focus of this paper is on the third d state, which is the only $\Lambda = \Pi$ state dissociating to $2S + 3P$ for which rovibrationally resolved spectra have been measured, but only 13 lines were observed (with $v = 6, 7, 8, 10$) [6]. Hyperfine structure was also studied experimentally for $3d$ in [8], but it was only for the $N = 6, 8$ levels of $v = 8$, which had already been studied without focus on hyperfine structure in [6]. Finally, the $3d$ state was involved in the experiments of [7], but the focus of that study was not the $3d$ state.

Since the $3d$ state has four spin-orbit daughter states ($0_g^+, 0_g^-, 1_g, 2_g$, analogous with the $3b$ state), we treat the 2_g symmetry in this paper, since there is only one state dissociating to $2S + 3P$ with 2_g symmetry and therefore the long-range potential is a simple sum of inverse-power terms rather than a complicated 2×2 or 3×3 interaction matrix. The fitting strategy was very similar to what it was for the $3C$ state, except the $3d$ state seemed to require stronger weighting of the points near the second minimum, and weaker weighting of other points. These final weights are shown in Table VI.

Once these final weights were chosen, fits were performed for 238 different combinations of the MLR parameters $(N_\beta, p, q, r_{\text{ref}})$, with $3 \leq N_\beta \leq 11$, $5 \leq p \leq 8$, $2 \leq q \leq 10$, ($5 \leq r_{\text{ref}} \leq 7.5$) Å, though not every point in the convex hull formed by these ranges was used, and it is noted that p must be ≥ 6 in order to ensure the correct long-range behavior [17], but fits with $p = 5$ were still instructive to better understand the model dependence for this potential. The best fit with $N_\beta = 4$ and $p \geq 6$ was with $(p, q, r_{\text{ref}}) = (6, 7, 7.2 \text{ Å})$ which had $dd = 4.292$, only 0.043 higher than the best fit found with $p = 5$. Fits with $N_\beta = 5$ had dd values as low as 2.972 but the mentioned $N_\beta = 4$ case did not misrepresent any of the original

points beyond 2.434 Å) by $> 13 \text{ cm}^{-1}$, so all desiderata were satisfied without resorting to $N_\beta = 5$. No $N_\beta = 3$ cases had $dd < 10$, so the choice of MLR model for this electronic state was easy to make, and the final parameters are listed in Table III.

III. CONCLUSION

Analytic MLR potentials were fitted to the *ab initio* points from [28] and with correct long-range behavior incorporated according to effects of spin-orbit coupling described in Eqs. 8, 10, 11 and the long-range constants in Table II. Despite the potentials from [28] having unusual features such as multiple minima, barriers, and shelves, which have never been described by an MLR-type model before, all of these features were successfully captured with the MLR model. This answers an age-old question of whether or not fully analytic potentials can have the flexibility needed in order to capture such features. Pashov’s 2008 paper “Pointwise and analytic potentials for diatomic molecules. An attempt for critical comparison” [54] described lack of flexibility as one of the three drawbacks of analytic potentials, and suggested that the MLR model may not be able to capture double minima or shelf-like features. Five years earlier in 2003, Huang and Le Roy suggested in [53] that Pashov’s pointwise approach would be the method of choice for potentials such as those described in this paper:

“A particular strength of [Pashov’s pointwise] model is the fact that it has more local flexibility than do fully analytical potential function forms, in that a shift of one potential point has only a modest effect on the function outside its immediate neighborhood. This would tend to make [Pashov’s pointwise] model the method of choice for cases where the potential has substantial local structure or undergoes an abrupt change of character on a small fraction of the overall interval, such as occurs near an avoided curve crossing. In contrast, a change in one of the parameters defining a [fully analytic] such as our DELR function will in general affect the potential across the whole domain. This makes the parameters defining [fully analytic] potentials very highly correlated and can give rise to difficulty in achieving full unique convergence in a fit.”

At the time when this quote was written, the MLR model did not exist yet, and at the time of Pashov’s paper [54], only a primitive (less flexible) form of the MLR existed, which was used in just four simple cases of ground electronic states [55–58]. It is possible that the notion that analytic potentials cannot capture such special features may be attributed to the lack of diversity in attempted applications at that early stage in time, and the lack of

some of the newer MLR features which were introduced in [18] and [48] for increasing flexibility, and in [47] for correcting the long-range behavior.

This paper also represents, to the best of my knowledge, the most detailed study of analytic potentials for excited electronic molecular states.

ACKNOWLEDGMENTS

I am indebted to Monique Aubert-Frécon for taking the time to look through her old notes to answer my request for advice on the analytic form for the long-range potentials at the $nS - n'P$ asymptotes of alkali dimers. I also thank Michael Bromley of The University of Queensland (Australia) for advice about the long-range constants at the $nS - n'P$ asymptote, and Robert J. Le Roy of University of Waterloo (Canada) for many helpful discussions.

Table IV. Quality of MLR_{6,7}^{5,9}(17) fit to original *ab initio* energies of [28] for the $3b(3^3\Pi_{2u})$ state. When an isotopologue listed in Table V has at least one vibrational energy level beyond the range of *ab initio* data available, approximate distances are given for the outer classical turning points of the corresponding vibrational wavefunctions.

r [Å]	Original [cm ⁻¹]	Weight [cm ⁻¹]	MLR - Original [cm ⁻¹]	MLR [cm ⁻¹]
2.328 380	-1 501.30	40.00	195.839	-1305.461
2.434 215	-2 661.44	40.00	9.542	-2651.898
2.540 051	-3 556.46	40.00	-79.794	-3636.254
2.645 886	-4 232.00	40.00	-104.149	-4336.149
2.751 721	-4 727.14	40.00	-89.498	-4816.638
2.857 557	-5 075.00	20.00	-57.523	-5132.523
2.963 392	-5 304.35	10.00	-25.034	-5329.384
3.069 228	-5 440.87	0.70	-2.753	-5443.623
3.175 063	-5 508.47	0.70	5.647	-5502.823
3.280 899	-5 530.85	0.70	3.179	-5527.671
3.386 734	-5 533.92	0.70	-1.971	-5535.891
3.492 570	-5 543.14	0.70	-2.801	-5545.941
3.598 405	-5 576.94	0.70	1.583	-5575.357
3.704 240	-5 634.66	0.70	3.546	-5631.114
3.810 076	-5 700.51	0.70	0.373	-5700.137
3.915 911	-5 750.55	0.70	-2.666	-5753.216
4.021 747	-5 761.08	0.70	-0.047	-5761.127
4.127 582	-5 708.41	0.90	2.634	-5705.776
4.233 418	-5 578.48	0.90	-0.382	-5578.862
4.339 253	-5 376.12	1.00	-3.307	-5379.427
4.445 089	-5 120.65	2.00	1.698	-5118.952
4.550 924	-4 832.92	4.00	9.143	-4823.777
4.656 759	-4 528.51	4.00	7.006	-4521.504
4.762 595	-4 217.95	4.00	-4.138	-4222.088
4.868 430	-3 908.28	4.00	-9.716	-3917.996
4.974 266	-3 603.65	1.00	-1.519	-3605.169
5.080 101	-3 307.57	3.00	10.262	-3297.308
5.185 937	-3 022.26	3.00	9.62	-3012.64
5.291 772	-2 749.45	1.00	-2.696	-2752.146
5.609 278	-2 018.82	1.00	1.364	-2017.456
5.820 949	-1 611.25	1.00	-2.927	-1614.177
6.138 456	-1 127.31	1.00	4.595	-1122.715
6.350 127	-958.32	0.30	-0.912	-959.232
6.667 633	-935.05	0.30	0.886	-934.164
6.879 304	-931.76	0.30	-1.386	-933.146
7.196 810	-925.40	0.30	1.252	-924.148
7.408 481	-917.28	0.30	-1.012	-918.292
7.725 987	-895.77	1.50	3.616	-892.154
7.937 658	-872.50	1.50	5.113	-867.387
8.255 164	-817.85	1.50	-2.201	-820.051
8.466 835	-764.30	4.00	-6.928	-771.228
8.784 342	-656.98	4.00	-5.076	-662.056
8.996 013	-572.26	4.00	9.21	-563.05
9.260 601	-464.06	4.00	8.64	-455.42
9.525 190	-364.42	4.00	8.00	-356.42
9.789 778	-280.36	4.00	7.29	-273.07
10.054 367	-213.64	4.00	6.54	-207.1
10.318 956	-163.16	4.00	5.78	-157.38
10.583 544	-125.85	2.00	5.04	-120.81
11.112 721	-78.44	2.00	4.35	-74.09
11.641 899	-52.11	2.00	3.69	-48.42
12.171 076	-36.52	2.00	3.16	-33.36
12.700 253	-26.43	2.00	2.72	-23.71
13.229 430	-19.84	2.00	2.37	-17.47
13.758 607	-15.24	5.50	2.09	-13.15
14.287 785	-11.94	5.50	1.88	-10.06
14.816 962	-9.53	5.50	1.71	-7.82
15.346 139	-7.55	5.00	1.53	-6.02
15.875 316	-6.24	5.00	1.37	-4.87
16.933 671	-4.04	5.00	1.21	-2.83
17.992 025	-2.73	5.00	1.08	-1.65
19.050 380	-1.85	5.00	0.96	-0.89
20.108 734	-1.19	5.00	0.86	-0.33
21.167 088	-0.75	0.50	0.73	-0.02
65.	-	-	-	-0.003
70.	-	-	-	-0.002

Table V. Vibrational energies in cm⁻¹ for the $3b(3^3\Pi_{2u})$ state predicted by the MLR_{6,7}^{5,9}(17) from Table III.

v	^{6,6} Li ₂	^{6,7} Li ₂	^{7,7} Li ₂	^{11,11} Li ₂
\mathcal{D}_e	5 765.593	5 765.593	5 765.593	5 765.593
0	-5 654.932	-5658.488	-5662.222	-5661.726
1	-5 493.765	-5500.003	-5506.570	-5505.696
2	-5 385.710	-5397.683	-5356.570	-5408.260
3	-5 241.269	-5260.427	-5280.073	-5277.492
4	-5 083.976	-5110.717	-5138.177	-5134.567
5	-4 914.852	-4980.180	-4984.997	-4980.318
6	-4 737.691	-4780.180	-4823.968	-4818.203
7	-4 554.829	-4605.151	-4657.110	-4650.263
8	-4 368.240	-4426.227	-4486.207	-4478.297
9	-4 179.292	-4244.786	-4312.615	-4303.664
10	-3 988.756	-4061.679	-4137.249	-4127.274
11	-3 796.972	-3877.308	-3960.593	-3949.597
12	-3 604.218	-3691.902	-3782.874	-3770.860
13	-3 411.033	-3505.823	-3604.333	-3591.316
14	-3 218.297	-3319.731	-3404.333	-3411.444
15	-3 027.108	-3134.538	-3246.854	-3231.976
16	-2 838.477	-2951.238	-3069.490	-3053.803
17	-2 652.930	-2770.592	-2894.177	-2877.765
18	-2 470.302	-2592.818	-2721.446	-2704.363
19	-2 290.105	-2417.585	-2551.310	-2533.558
20	-2 112.256	-2244.505	-2383.395	-2364.958
21	-1 937.405	-2073.700	-2217.430	-2198.327
22	-1 766.631	-1905.899	-2053.644	-2033.962
23	-1 600.818	-1742.086	-1892.754	-1872.628
24	-1 440.124	-1582.955	-1735.630	-1715.198
25	-1 284.340	-1428.527	-1582.844	-1562.186
26	-1 134.583	-1278.624	-1434.376	-1413.503
27	-996.778	-1134.368	-1290.038	-1269.027
28	-914.777	-1001.099	-1150.711	-1129.946
29	-882.576	-916.881	-1020.440	-1001.313
30	-845.026	-887.471	-950.440	-918.124
31	-800.327	-851.265	-898.383	-890.415
32	-753.924	-830.000	-861.863	-813.832
33	-705.900	-808.055	-820.356	-813.832
34	-654.935	-718.573	-780.226	-772.047
35	-602.077	-669.908	-737.158	-728.415
36	-548.234	-619.419	-690.970	-681.806
37	-493.706	-567.885	-643.224	-633.418
38	-438.926	-515.524	-594.281	-583.945
39	-384.474	-462.746	-544.287	-533.563
40	-330.903	-410.071	-493.717	-482.653
41	-278.814	-357.964	-443.010	-431.682
42	-228.913	-306.931	-392.539	-381.054
43	-182.018	-257.565	-342.733	-331.205
44	-139.060	-210.538	-362.733	-282.642
45	-101.066	-166.620	-247.119	-235.929
46	-69.047	-126.682	-202.462	-191.711
47	-43.749	-91.656	-160.811	-150.725
48	-25.299	-62.409	-122.952	-113.784
49	-13.022	-39.497	-89.714	-81.728
50	-5.669	-22.881	-61.855	-55.277
51	-1.855	-11.834	-39.854	-34.795
52	-0.324	-5.193	-23.675	-20.079
53	-0.002	-1.723	-12.691	-10.348
54	-	-0.312	-5.885	-4.517
55	-	-0.003	-3.885	-1.482
56	-	-	-0.493	-0.261
57	-	-	-	-0.002

Table VI. Quality of $\text{MLR}_{6,6}^{6,2}(4)$ fit to original *ab initio* energies of [28] for the $3B(3^1\Pi_{1u})$. When an isotopologue listed in Table VII has at least one vibrational energy level beyond the range of *ab initio* data available, approximate distances are given for the outer classical turning points of the corresponding vibrational wavefunctions.

r [Å]	Original [cm^{-1}]	Weight [cm^{-1}]	MLR - Original [cm^{-1}]	MLR [cm^{-1}]
2.223	-305.82	100	798.584	492.764
2.328	-1574.16	100	354.615	-1219.545
2.434	-2650.69	100	133.127	-2517.563
2.540	-3531.22	100	45.218	-3486.002
2.646	-4198.64	1.00	5.965	-4192.675
2.752	-4684.78	1.00	-7.168	-4691.948
2.858	-5020.35	1.00	-7.054	-5027.404
2.963	-5232.81	1.00	-1.234	-5234.044
3.069	-5344.96	1.00	5.069	-5339.891
3.175	-5375.90	1.00	8.448	-5367.452
3.281	-5342.54	1.00	7.751	-5334.789
3.387	-5259.14	1.00	2.771	-5256.369
3.493	-5140.19	1.00	-3.585	-5143.775
3.598	-4997.31	1.00	-8.898	-5006.208
3.704	-4841.04	1.00	-9.908	-4850.948
3.810	-4677.75	1.00	-5.925	-4683.675
3.916	-4509.20	1.00	0.439	-4508.761
4.022	-4335.59	1.00	6.090	-4329.500
4.128	-4157.16	1.00	8.759	-4148.401
4.233	-3975.87	1.00	8.547	-3967.323
4.339	-3793.49	1.00	5.762	-3787.728
4.445	-3612.64	1.00	1.858	-3610.782
4.551	-3435.53	1.00	-2.007	-3437.537
4.657	-3264.12	1.00	-4.836	-3268.956
4.763	-3099.95	1.00	-6.043	-3105.993
4.868	-2943.90	1.00	-5.667	-2949.567
4.974	-2796.86	1.00	-3.664	-2800.524
5.080	-2658.59	1.00	-0.931	-2659.521
5.186	-2529.32	1.00	2.311	-2527.009
5.292	-2407.73	1.00	4.610	-2403.120
5.609	-2085.10	1.00	5.795	-2079.305
5.821	-1895.91	1.00	1.938	-1893.972
6.138	-1632.98	1.00	-3.702	-1636.682
6.350	-1462.67	1.00	-4.605	-1467.275
6.668	-1209.84	1.00	-1.783	-1211.623
6.879	-1046.55	1.00	0.657	-1045.893
7.197	-822.68	1.00	3.489	-819.191
7.408	-692.97	1.00	3.915	-689.055
7.726	-532.10	1.00	3.269	-528.831
7.938	-445.62	1.00	1.783	-443.837
8.255	-343.13	1.00	-0.567	-343.697
8.467	-289.80	1.00	-1.852	-291.652
8.784	-227.03	1.00	-3.294	-230.324
8.996	-194.11	1.00	-3.988	-198.098
9.261	-160.97	1.00	-4.249	-165.219
9.525	-134.41	1.00	-4.343	-138.753
9.790	-113.12	1.00	-4.130	-117.250
10.054	-96.00	1.00	-3.622	-99.622
10.319	-81.96	1.00	-3.106	-85.066
10.584	-70.10	1.00	-2.845	-72.945
11.113	-52.33	1.00	-1.958	-54.288
11.642	-39.60	1.00	-1.360	-40.960
12.171	-30.38	1.00	-0.904	-31.284
12.700	-23.58	1.00	-0.585	-24.165
13.229	-18.53	1.00	-0.326	-18.856
13.759	-14.58	1.00	-0.287	-14.867
14.288	-11.72	1.00	-0.128	-11.848
14.817	-9.31	1.00	-0.232	-9.542
15.346	-7.55	1.00	-0.189	-7.739
15.875	-6.24	1.00	-0.093	-6.333
16.934	-4.04	1.00	-0.275	-4.315
17.992	-2.73	1.00	-0.292	-3.022
19.050	-1.85	1.00	-0.310	-2.160
20.109	-1.19	1.00	-0.385	-1.575
21.167	-0.75	0.50	-0.421	-1.171

Table VII. Vibrational energies in cm^{-1} for the $3B(3^1\Pi_{1u})$ state predicted by the $\text{MLR}_{6,6}^{6,2}(4)$ from Table III.

v	$^{6,6}\text{Li}_2$	$^{6,7}\text{Li}_2$	$^{7,7}\text{Li}_2$	$^{11,11}\text{Li}_2$
\mathcal{D}_e	5368.8	5368.8	5368.8	5368.8
0	-5259.702	-5263.694	-5267.840	-5267.292
1	-5047.141	-5058.712	-5070.746	-5069.155
2	-4838.570	-4857.433	-4877.067	-4874.470
3	-4634.049	-4659.912	-4686.855	-4683.290
4	-4433.598	-4466.170	-4500.132	-4495.636
5	-4237.212	-4276.205	-4316.896	-4311.508
6	-4044.874	-4090.002	-4137.136	-4130.892
7	-3856.578	-3907.553	-3960.843	-3953.781
8	-3672.341	-3728.865	-3788.017	-3780.174
9	-3492.217	-3553.977	-3618.683	-3610.100
10	-3316.304	-3382.962	-3452.895	-3443.613
11	-3144.757	-3215.941	-3290.743	-3280.808
12	-2977.780	-3053.079	-3132.356	-3121.818
13	-2815.625	-2894.584	-2977.902	-2966.817
14	-2658.578	-2740.700	-2827.582	-2816.010
15	-2506.934	-2591.690	-2681.624	-2669.630
16	-2360.954	-2447.812	-2540.262	-2527.916
17	-2220.808	-2309.273	-2403.714	-2391.085
18	-2086.496	-2176.175	-2272.140	-2259.292
19	-1957.783	-2048.452	-2145.593	-2132.577
20	-1834.183	-1925.822	-2023.966	-2010.813
21	-1715.028	-1807.793	-1906.966	-1893.682
22	-1599.606	-1693.743	-1794.128	-1780.695
23	-1487.302	-1583.044	-1684.891	-1671.279
24	-1377.678	-1475.167	-1578.702	-1564.878
25	-1270.487	-1369.744	-1475.101	-1461.040
26	-1165.652	-1266.570	-1373.763	-1359.458
27	-1063.233	-1165.583	-1274.505	-1259.962
28	-963.397	-1066.840	-1177.266	-1162.507
29	-866.401	-970.488	-1082.087	-1067.149
30	-772.574	-876.755	-989.090	-974.022
31	-682.312	-785.929	-898.465	-883.330
32	-596.065	-698.356	-810.456	-795.329
33	-514.332	-614.434	-725.359	-710.329
34	-437.645	-534.599	-643.512	-628.681
35	-366.550	-459.324	-565.294	-550.774
36	-301.572	-389.096	-491.112	-477.030
37	-243.166	-324.395	-421.395	-407.885
38	-191.657	-265.654	-356.577	-343.778
39	-147.184	-213.218	-297.065	-285.115
40	-109.665	-167.284	-243.214	-232.239
41	-78.804	-127.871	-195.278	-185.379
42	-54.137	-94.805	-153.373	-144.621
43	-35.092	-67.741	-117.455	-109.880
44	-21.035	-46.216	-87.316	-80.910
45	-11.285	-29.692	-62.618	-57.343
46	-5.113	-17.586	-42.931	-38.724
47	-1.738	-9.275	-27.767	-24.548
48	-0.325	-4.092	-16.603	-14.276
49	-0.007	-1.326	-8.884	-8.884
50		-0.222	-4.015	-4.015
51		-0.003	-1.362	-7.331
52			-0.256	-3.100
53			-0.007	-0.929

Table VIII. Quality of MLR_{6,8}^{7,0}(8) fit to original *ab initio* energies of [28] for the 3C(3¹Π_{1g}) state.

r [Å]	Original [cm ⁻¹]	Weight [cm ⁻¹]	MLR - Original [cm ⁻¹]	MLR [cm ⁻¹]
2.328	-331.50	10.00	35.693	-295.807
2.434	-1429.53	10.00	-7.764	-1437.294
2.540	-2276.70	10.00	-22.184	-2298.884
2.645	-2916.47	10.00	-20.557	-2937.027
2.751	-3385.05	5.00	-11.667	-3396.717
2.857	-3712.29	5.00	-1.457	-3713.747
2.963	-3915.52	5.00	-0.992	-3916.512
3.069	-4031.62	5.00	4.084	-4027.536
3.175	-4078.81	5.00	14.101	-4064.709
3.280	-4049.18	5.00	6.865	-4042.315
3.386	-3981.36	5.00	9.450	-3971.910
3.492	-3867.67	5.00	4.697	-3862.973
3.598	-3723.48	5.00	0.049	-3723.431
3.704	-3556.02	5.00	-3.998	-3560.018
3.810	-3371.66	5.00	-6.935	-3378.595
3.915	-3176.11	5.00	-8.227	-3184.337
4.021	-2973.97	5.00	-7.885	-2981.855
4.127	-2768.98	5.00	-6.346	-2775.326
4.233	-2564.65	5.00	-3.854	-2568.504
4.339	-2364.05	5.00	-0.696	-2364.746
4.445	-2169.38	5.00	2.391	-2166.989
4.550	-1982.83	5.00	5.140	-1977.690
4.656	-1805.27	5.00	6.500	-1798.770
4.762	-1638.69	5.00	7.099	-1631.591
4.868	-1483.30	5.00	6.415	-1476.885
4.974	-1339.76	5.00	4.958	-1334.802
5.080	-1208.08	5.00	3.099	-1204.981
5.185	-1087.37	5.00	0.726	-1086.644
5.291	-977.63	1.00	-1.168	-978.798
5.609	-707.90	1.00	-0.784	-708.684
5.820	-568.75	1.00	1.689	-567.061
6.138	-405.90	1.00	0.725	-405.175
6.350	-320.52	1.00	-2.067	-322.587
6.667	-218.69	1.00	-0.594	-219.284
6.879	-166.01	1.00	2.617	-163.393
7.196	-109.83	1.00	1.706	-108.124
7.408	-88.76	0.50	-1.103	-89.863
7.725	-80.64	0.50	-0.478	-81.118
7.937	-82.83	0.50	0.689	-82.141
8.255	-87.00	0.50	0.527	-86.473
8.466	-88.32	0.50	-0.061	-88.381
8.784	-87.44	0.50	-0.480	-87.920
8.996	-85.25	1.00	-0.356	-85.606
9.260	-81.08	1.00	-0.110	-81.190
9.525	-76.03	1.00	0.225	-75.805
9.789	-70.32	1.00	0.334	-69.986
10.054	-64.40	1.00	0.321	-64.079
10.318	-58.47	1.00	0.196	-58.274
10.583	-52.98	1.00	0.266	-52.714
11.112	-42.67	1.00	0.025	-42.645
11.641	-34.11	1.00	-0.050	-34.160
12.171	-27.09	1.00	-0.159	-27.249
12.700	-21.60	1.00	-0.120	-21.720
13.229	-17.21	1.00	-0.140	-17.350
13.758	-13.92	1.00	-0.003	-13.923
14.287	-11.28	1.00	0.034	-11.246
14.816	-9.09	1.00	-0.061	-9.151
15.346	-7.33	1.00	-0.151	-7.481
15.875	-6.02	1.00	-0.140	-6.160
16.933	-4.04	1.00	-0.194	-4.234
17.992	-2.73	1.00	-0.253	-2.983
19.050	-1.85	1.00	-0.290	-2.140
20.108	-0.75	0.50	-0.415	-1.165

Table IX. Vibrational energies in cm⁻¹ for the 3C(3¹Π_{1g}) state predicted by the MLR_{6,8}^{7,0}(8) from Table III.

v	^{6,6} Li ₂	^{6,7} Li ₂	^{7,7} Li ₂	^{11,11} Li ₂
\mathcal{D}_e				
0	-3957.890	-3961.862	-3965.987	-3965.442
1	-3745.119	-3761.862	-3765.987	-3765.442
2	-3445.119	-3552.904	-3572.894	-3570.251
3	-3324.020	-3350.648	-3378.354	-3374.690
4	-3116.570	-3150.393	-3185.613	-3180.954
5	-2911.754	-2952.521	-2995.010	-2989.387
6	-2710.006	-2757.416	-2806.885	-2800.335
7	-2511.771	-2565.475	-2606.885	-2600.335
8	-2317.519	-2377.112	-2439.475	-2431.207
9	-2127.744	-2192.761	-2260.933	-2251.888
10	-1942.968	-2092.761	-2086.359	-2076.600
11	-1763.742	-1837.961	-1916.175	-1905.775
12	-1590.632	-1668.499	-1750.820	-1739.859
13	-1424.202	-1505.005	-1590.747	-1579.313
14	-1264.977	-1347.972	-1436.402	-1424.589
15	-1113.398	-1197.836	-1288.205	-1276.109
16	-969.785	-1054.947	-1188.205	-1134.234
17	-834.340	-919.540	-1011.602	-934.234
18	-707.248	-791.774	-883.647	-871.271
19	-588.846	-671.841	-762.784	-750.496
20	-479.738	-560.115	-649.211	-637.121
21	-380.571	-457.196	-543.311	-531.558
22	-291.279	-363.593	-445.642	-434.379
23	-210.843	-279.026	-356.603	-345.930
24	-179.563	-202.533	-275.840	-265.738
25	-139.563	-134.770	-202.474	-192.963
26	-75.962	-95.896	-137.129	-128.680
27	-59.183	-75.896	-107.129	-108.680
28	-44.917	-59.831	-77.432	-75.195
29	-32.408	-45.935	-57.432	-60.065
30	-23.147	-33.705	-48.506	-46.489
31	-13.147	-23.705	-36.508	-36.489
32	-6.897	-14.533	-25.881	-24.164
33		-8.064	-17.012	-15.608
34		-3.706	-10.101	-9.034
35			-5.173	-4.447

Table X. Quality of MLR_{6,9}^{7,2}(4) fit to original *ab initio* energies of [28] for the $3d(3^3\Pi_g)$ state. When an isotopologue listed in Table XI has at least one vibrational energy level beyond the range of *ab initio* data available, approximate distances are given for the outer classical turning points of the corresponding vibrational wavefunctions.

r [Å]	Original [cm ⁻¹]	Weight [cm ⁻¹]	MLR - Original [cm ⁻¹]	MLR [cm ⁻¹]
2.222544	-675.63	150.00	242.061	-433.569
2.328380	-2176.84	15.00	96.978	-2079.862
2.434215	-3353.22	10.00	27.796	-3325.424
2.540051	-4256.36	1.00	1.853	-4254.507
2.645886	-4929.71	1.00	-3.720	-4933.430
2.751721	-5412.99	1.00	-1.158	-5414.148
2.857557	-5739.79	1.00	2.660	-5737.130
2.963392	-5939.29	1.00	5.574	-5933.716
3.069228	-6034.33	1.00	6.128	-6028.202
3.175063	-6043.98	1.00	4.493	-6039.487
3.280899	-5986.48	1.00	3.904	-5982.576
3.386734	-5867.31	1.00	-2.283	-5869.593
3.492570	-5704.90	1.00	-5.728	-5710.628
3.598405	-5506.27	1.00	-8.024	-5514.294
3.704240	-5278.46	1.00	-9.647	-5288.107
3.810076	-5028.69	1.00	-9.954	-5038.644
3.915911	-4762.69	10.00	-9.071	-4771.761
4.021747	-4485.27	10.00	-7.326	-4492.596
4.127582	-4200.62	10.00	-5.101	-4205.721
4.233418	-3912.45	10.00	-2.679	-3915.129
4.339253	-3624.06	10.00	-0.318	-3624.378
4.445089	-3338.52	1.00	1.889	-3336.631
4.550924	-3058.47	1.00	3.726	-3054.744
4.656759	-2786.32	1.00	5.015	-2781.305
4.762595	-2524.27	1.00	5.575	-2518.695
4.868430	-2274.73	1.00	5.652	-2269.078
4.974266	-2039.01	1.00	4.615	-2034.395
5.080101	-1819.10	1.00	2.755	-1816.345
5.185937	-1616.52	1.00	0.247	-1616.273
5.291772	-1432.60	1.00	-2.570	-1435.17
5.609278	-997.82	1.00	-10.897	-1008.717
5.820949	-804.90	1.00	-12.271	-817.171
6.138456	-638.54	1.00	-6.685	-645.225
6.350127	-587.84	0.10	-1.544	-589.384
6.667633	-563.92	0.10	1.767	-562.153
6.879304	-564.36	0.10	0.378	-563.982
7.196810	-570.07	0.10	-1.508	-571.578
7.408481	-570.51	0.10	-0.877	-571.387
7.725987	-559.75	0.10	1.099	-558.651
7.937658	-543.07	1.00	1.662	-541.408
8.466835	-466.48	1.00	0.547	-465.933
8.784342	-401.07	1.00	-1.351	-402.421
8.996013	-353.88	1.00	-3.111	-356.991
9.260601	-296.16	1.00	-5.093	-301.253
9.525190	-243.05	1.00	-7.119	-250.169
9.789778	-197.62	1.00	-8.143	-205.763
10.054367	-160.09	1.00	-8.449	-168.539
10.318956	-129.80	1.00	-8.245	-138.045
10.583544	-105.88	1.00	-7.519	-113.399
11.112721	-72.08	1.00	-5.612	-77.692
11.641899	-50.57	1.00	-3.992	-54.562
12.171076	-36.52	1.00	-2.767	-39.287
12.700253	-26.87	1.00	-2.082	-28.952
13.229430	-20.50	1.00	-1.257	-21.757
13.758607	-15.67	1.00	-0.966	-16.636
14.287785	-12.38	1.00	-0.534	-12.914
14.816962	-9.75	1.00	-0.406	-10.156
15.346139	-7.77	1.00	-0.300	-8.070
15.875316	-6.24	1.00	-0.245	-6.485
16.933671	-4.04	1.00	-0.243	-4.283
17.992025	-2.73	1.00	-0.189	-2.919
19.050380	-1.85	1.00	-0.181	-2.031
20.108734	-1.19	1.00	-0.251	-1.441
21.167088	-0.75	0.50	-0.290	-1.040
21.5	—	—	—	-0.964
23.	—	—	—	-0.608

Table XI. Vibrational energies in cm⁻¹ for the $3d(3^3\Pi_g)$ state predicted by the MLR_{6,9}^{7,2}(4) from Table III.

v	^{6,6} Li ₂	^{6,7} Li ₂	^{7,7} Li ₂	^{11,11} Li ₂
\mathcal{D}_e	6 045.135	6 045.135	6 045.135	6 045.135
0	-5909.082	-5914.058	-5919.226	-5918.543
1	-5641.796	-5656.375	-5671.532	-5669.528
2	-5377.524	-5401.482	-5371.532	-5369.528
3	-5116.452	-5149.547	-5183.994	-5179.438
4	-4858.751	-4949.547	-4944.436	-4938.652
5	-4604.574	-4655.149	-4707.858	-4700.882
6	-4354.070	-4412.959	-4474.377	-4466.246
7	-4107.378	-4174.278	-4244.107	-4234.860
8	-3864.636	-3939.232	-4017.158	-4006.835
9	-3625.987	-3707.944	-3793.641	-3782.284
10	-3391.579	-3480.547	-3573.669	-3561.322
11	-3161.574	-3257.179	-3357.363	-3344.073
12	-2936.152	-3037.995	-3144.853	-3130.670
13	-2715.518	-2823.167	-2936.284	-2921.261
14	-2499.912	-2612.894	-2731.819	-2716.013
15	-2289.614	-2407.408	-2531.648	-2515.121
16	-2084.961	-2206.980	-2331.648	-2318.811
17	-1886.358	-2011.936	-2145.098	-2118.811
18	-1694.302	-1822.668	-1959.285	-1941.046
19	-1509.404	-1639.650	-1778.914	-1760.288
20	-1332.434	-1463.471	-1604.431	-1585.534
21	-1164.385	-1294.865	-1436.381	-1417.351
22	-1006.574	-1134.778	-1275.444	-1256.450
23	-860.858	-984.465	-1122.490	-1103.740
24	-730.125	-845.692	-978.663	-960.432
25	-620.025	-721.209	-845.563	-828.230
26	-600.025	-616.435	-725.642	-709.810
27	-536.279	-586.435	-623.550	-610.540
28	-502.410	-537.243	-582.928	-576.909
29	-464.979	-505.003	-542.928	-536.909
30	-425.955	-469.139	-511.362	-506.341
31	-380.025	-431.738	-477.652	-476.341
32	-344.186	-411.738	-442.209	-435.772
33	-302.862	-353.180	-405.126	-398.323
34	-262.005	-313.325	-367.188	-360.082
35	-222.176	-273.774	-328.906	-321.577
36	-183.954	-235.025	-290.723	-283.260
37	-163.228	-197.591	-253.083	-245.580
38	-113.198	-162.009	-216.432	-208.993
39	-104.815	-128.846	-181.237	-173.977
40	-79.439	-98.692	-117.188	-150.689
41	-39.669	-69.707	-107.188	-110.689
42	-23.171	-49.707	-84.675	-90.404
43	-12.113	-31.768	-64.675	-70.404
44	-5.236	-18.400	-44.675	-40.404
45	-1.618	-9.302	-28.485	-25.161
46	—	-3.816	-16.488	-20.161
47	—	-1.061	-8.348	-6.813
48	—	—	-3.439	-2.591
49	—	—	-0.964	-0.608

-
- [1] X. Xie and R. Field, *Journal of Molecular Spectroscopy* **117**, 228 (1986).
- [2] A. Yiannopoulou, K. Urbanski, A. M. Lyyra, L. Li, B. Ji, J. T. Bahns, and W. C. Stwalley, *The Journal of Chemical Physics* **102**, 3024 (1995).
- [3] D. Li, F. Xie, L. Li, A. Lazoudis, and A. M. Lyyra, *Journal of Molecular Spectroscopy* **246**, 180 (2007).
- [4] R. A. Bernheim, L. P. Gold, and T. Tipton, *The Journal of Chemical Physics* **78**, 3635 (1983).
- [5] M. Song, P. Yi, X. Dai, Y. Liu, L. Li, and G.-H. Jeung, *Journal of Molecular Spectroscopy* **215**, 251 (2002).
- [6] A. Yiannopoulou, K. Urbanski, S. Antonova, A. M. Lyyra, L. Li, T. An, T. J. Whang, B. Ji, X. T. Wang, W. C. Stwalley, T. Leininger, and G.-H. Jeung, *The Journal of Chemical Physics* **103**, 5898 (1995).
- [7] L. Li, S. Antonova, A. Yiannopoulou, K. Urbanski, and A. M. Lyyra, *The Journal of Chemical Physics* **105**, 9859 (1996).
- [8] L. Li, A. Yiannopoulou, K. Urbanski, A. M. Lyyra, B. Ji, W. C. Stwalley, and T. An, *The Journal of Chemical Physics* **105**, 6192 (1996).
- [9] V. Ivanov, V. Sovkov, L. Li, A. Lyyra, G. Lazarov, and J. Huennekens, *Journal of molecular spectroscopy* **194**, 147 (1999).
- [10] J. Sebastian, C. Gross, K. Li, H. C. J. Gan, W. Li, and K. Dieckmann, *Physical Review A* **90**, 033417 (2014).
- [11] M. Semczuk, X. Li, W. Gunton, M. Haw, N. S. Dattani, J. Witz, A. K. Mills, D. J. Jones, and K. W. Madison, *Physical Review A* **87**, 052505 (2013).
- [12] W. Gunton, M. Semczuk, N. Dattani, and K. Madison, *Physical Review A* **88**, 062510 (2013).
- [13] L.-Y. Tang, Z.-C. Yan, T.-Y. Shi, and J. Mitroy, *Physical Review A* **84** (2011), 10.1103/PhysRevA.84.052502.
- [14] J. Mitroy, M. S. Safronova, and C. W. Clark, *Journal of Physics B: Atomic, Molecular and Optical Physics* **43**, P02001 (2010).
- [15] A. D. Cronin, J. Schmiedmayer, and D. E. Pritchard, *Reviews of Modern Physics* **81**, 1051 (2009).
- [16] N. S. Dattani and R. J. LeRoy, *Journal of Chemical Physics* (2015).
- [17] N. S. Dattani and R. J. Le Roy, *Journal of Molecular Spectroscopy* **268**, 199 (2011).
- [18] R. J. Le Roy, N. S. Dattani, J. A. Coxon, A. J. Ross, P. Crozet, and C. Linton, *The Journal of Chemical Physics* **131**, 204309 (2009).
- [19] M. Aubert-Frécon, G. Hadinger, S. Magnier, and S. Rousseau, *Journal of Molecular Spectroscopy* **188**, 182 (1998).
- [20] B. Busser and M. Aubert-Frécon, *The Journal of Chemical Physics* **82**, 3224 (1985).
- [21] M. Aubert-Frécon, Private Communication (2015).
- [22] R. C. Brown, S. Wu, J. V. Porto, C. J. Sansonetti, C. E. Simien, S. M. Brewer, J. N. Tan, and J. D. Gillaspay, *Physical Review A* **87**, 032504 (2013).
- [23] C. J. Sansonetti, C. E. Simien, J. D. Gillaspay, J. N. Tan, S. M. Brewer, R. C. Brown, S. Wu, and J. V. Porto, *Physical Review Letters* **107**, 023001 (2011).
- [24] C. Sansonetti, B. Richou, R. Engleman, and L. Radziemski, *Physical Review A* **52**, 2682 (1995).
- [25] I. Schmidt-Mink, W. Müller, and W. Meyer, *Chemical Physics* **92**, 263 (1985).
- [26] R. Poteau and F. Spiegelmann, *Journal of Molecular Spectroscopy* **171**, 299 (1995).
- [27] P. Jasik and J. Sienkiewicz, *Chemical Physics* **323**, 563 (2006).
- [28] M. Musial and S. A. Kucharski, *Journal of Chemical Theory and Computation* **10**, 1200 (2014).
- [29] C.-W. Lee, *Bulletin of the Korean Chemical Society* **35**, 1422 (2014).
- [30] S. Bubin, M. Stanke, and L. Adamowicz, *The Journal of chemical physics* **131**, 044128 (2009).
- [31] N. S. Dattani, *Journal of Molecular Spectroscopy* **311**, 76 (2015).
- [32] S. Bubin and L. Adamowicz, *The Journal of Chemical Physics* **126**, 214305 (2007).
- [33] J. Koput, *The Journal of chemical physics* **135**, 244308 (2011).
- [34] J. Komasa, K. Piszczatowski, G. Lach, M. Przybytek, B. Jeziorski, and K. Pachucki, *Journal of Chemical Theory and Computation* **7**, 3105 (2011).
- [35] K. Pachucki and J. Komasa, *The Journal of chemical physics* **137**, 204314 (2012).
- [36] J. Noga and R. J. Bartlett, *The Journal of Chemical Physics* **86**, 7041 (1987).
- [37] S. Hirata and R. J. Bartlett, *Chemical Physics Letters* **321**, 216 (2000).
- [38] M. Kallay and P. R. Surjan, *The Journal of Chemical Physics* **115**, 2945 (2001).
- [39] M. Kallay and J. Gauss, *The Journal of chemical physics* **120**, 6841 (2004).
- [40] F. A. Evangelista, W. D. Allen, and H. F. Schaefer, *The Journal of chemical physics* **125**, 154113 (2006).
- [41] N. J. DeYonker and W. D. Allen, *The Journal of chemical physics* **137**, 234303 (2012).
- [42] N. J. DeYonker and S. A. Shah, *Theoretical Chemistry Accounts* **133**, 1518 (2014).
- [43] R. J. LeRoy, *Molecular Spectroscopy Molecular Spectroscopy*, **1**, 113 (1973).
- [44] R. J. LeRoy, *Canadian Journal of Physics* **52**, 246 (1974).
- [45] B. Ji, C.-C. Tsai, and W. C. Stwalley, *Chemical Physics Letters* **236**, 242 (1995).
- [46] J.-Y. Zhang, J. Mitroy, and M. Bromley, *Physical Review A* **75** (2007), 10.1103/PhysRevA.75.042509.
- [47] N. S. Dattani, R. J. LeRoy, A. J. Ross, and C. Linton, in *Proceedings of the International Symposium on Molecular Spectroscopy* (2008) p. RC11.
- [48] R. J. Le Roy, C. C. Haugen, J. Tao, and H. Li, *Molecular Physics* **109**, 435 (2011).
- [49] L.-Y. Tang, Z.-C. Yan, T.-Y. Shi, and J. Babb, *Physical Review A* **79** (2009), 10.1103/PhysRevA.79.062712.
- [50] L.-Y. Tang, Private Communication (2015).
- [51] L.-Y. Tang, Z.-C. Yan, T.-Y. Shi, and J. Mitroy, *Physical Review A* **81** (2010), 10.1103/PhysRevA.81.042521.
- [52] M. Marinescu and A. Dalgarno, *Physical Review A* **52**, 311 (1995).
- [53] Y. Huang and R. J. Le Roy, *The Journal of Chemical Physics* **119**, 7398 (2003).
- [54] A. Pashov, *Proceedings of the International Symposium on Molecular Spectroscopy*
- [55] R. J. Le Roy, Y. Huang, and C. Jary, *The Journal of Chemical Physics* **125**, 164310 (2006).
- [56] R. J. L. Roy and R. D. E. Henderson, *Molecular Physics* **105**, 663 (2007).

- [57] H. Salami, A. J. Ross, P. Crozet, W. Jas-trzebski, P. Kowalczyk, and R. J. Le Roy, *The Journal of Chemical Physics* **126**, 194313 (2007).
- [58] A. Shayesteh, R. D. E. Henderson, R. J. Le Roy, and P. F. Bernath, *The Journal of Physical Chemistry. A* **111**, 12495 (2007).
- [59] J. A. Coxon and P. G. Hajigeorgiou, *The Journal of Chemical Physics* **132**, 094105 (2010).
- [60] A. Stein, H. Knöckel, and E. Tiemann, *The European Physical Journal D* **57**, 171 (2010).
- [61] L. Piticco, F. Merkt, A. A. Cholewin-ski, F. R. McCourt, and R. J. Le Roy, *Journal of Molecular Spectroscopy* **264**, 83 (2010).
- [62] M. Ivanova, A. Stein, A. Pashov, A. V. Stolyarov, H. Knöckel, and E. Tiemann, *The Journal of Chemical Physics* **135**, 174303 (2011).
- [63] F. Xie, L. Li, D. Li, V. B. Sovkov, K. V. Mi-naev, V. S. Ivanov, A. M. Lyyra, and S. Magnier, *The Journal of Chemical Physics* **135**, 024303 (2011).
- [64] T. Yukiya, N. Nishimiya, Y. Samejima, K. Yamaguchi, M. Suzuki, C. D. Boone, I. Ozier, and R. J. Le Roy, *Journal of Molecular Spectroscopy* **283**, 32 (2013).
- [65] H. Knöckel, S. Rühmann, and E. Tiemann, *The Journal of Chemical Physics* **138**, 094303 (2013).
- [66] L. Wang, D. Xie, R. J. Le Roy, and P.-N. Roy, *The Journal of Chemical Physics* **139**, 034312 (2013).
- [67] G. Li, I. E. Gordon, P. G. Hajigeor-giou, J. A. Coxon, and L. S. Rothman, *Journal of Quantitative Spectroscopy and Radiative Transfer* **130**, 2814 (2013).
- [68] V. V. Meshkov, A. V. Stolyarov, M. C. Heaven, C. Haugen, and R. J. LeRoy, *The Journal of Chemical Physics* **140**, 064315 (2014).
- [69] N. S. Dattani, physics.chem-ph, arXiv:1408.3301 (2014).
- [70] J. A. Coxon and P. G. Hajigeorgiou, *Journal of Quantitative Spectroscopy and Radiative Transfer* **135**, 133 (2015).
- [71] S.-D. Walji, K. M. Sentjens, and R. J. Le Roy, *The Journal of chemical physics* **142**, 044305 (2015).
- [72] N. S. Dattani, L. N. Zack, M. Sun, E. R. Johnson, R. J. Le Roy, and L. M. Ziurys, physics.chem-ph, arXiv:1408.2276 (2014).
- [73] K.-L. Xiao, C.-L. Yang, M.-S. Wang, X.-G. Ma, and W.-W. Liu, *Journal of Quantitative Spectroscopy and Radiative Transfer* **102**, 2918 (2013).
- [74] K.-L. Xiao, C.-L. Yang, M.-S. Wang, X.-G. Ma, and W.-W. Liu, *The Journal of chemical physics* **139**, 074305 (2013).
- [75] D. Kedziera, L. Mentel, P. S. Zuchowski, and S. Knoop, *Physical Review A* **91**, 062711 (2015).
- [76] T. Q. Teodoro, R. L. A. Haiduke, U. Dammalapati, S. Knoop, and L. Visscher, *The Journal of Chemical Physics* **143**, 084307 (2015).
- [77] Y. You, C.-L. Yang, M.-S. Wang, X.-G. Ma, W.-W. Liu, and L.-Z. Wang, *Journal of Quantitative Spectroscopy and Radiative Transfer* **165**, 616 (2015).
- [78] Y. You, C.-L. Yang, M.-S. Wang, X.-G. Ma, W.-W. Liu, and L.-Z. Wang, *Spectrochimica Acta Part A: Molecular and Biomolecular Spectroscopy*, (2015) [10.1016/j.saa.2015.09.041](https://doi.org/10.1016/j.saa.2015.09.041).
- [79] Y. You, C.-L. Yang, M.-S. Wang, X.-G. Ma, and W.-W. Liu, *Physical Review A* **92**, 032502 (2015).
- [80] H. Li and R. J. Le Roy, *Physical Chemistry Chemical Physics : PCCP* **10**, 4128 (2008).
- [81] H. Li, P.-N. Roy, and R. J. Le Roy, *The Journal of Chemical Physics* **133**, 104305 (2010).
- [82] Y. Tritzant-Martinez, T. Zeng, A. Broom, E. Meiering, R. J. Le Roy, and P.-N. Roy, *The Journal of Chemical Physics* **138**, 234103 (2013).
- [83] H. Li, X.-L. Zhang, R. J. Le Roy, and P.-N. Roy, *The Journal of Chemical Physics* **139**, 164315 (2013).
- [84] Y.-T. Ma, T. Zeng, and H. Li, *The Journal of chemical physics* **140**, 214309 (2014).
- [85] R. J. Le Roy, J. Y. Seto, and Y. Huang, "DPotFit 2.0: A Computer Program for Fitting Diatomic Molecule Spectra to Potential Energy Functions (University of Waterloo Chemical Physics Research Report CP-667)," (2013).
- [86] F. Engelke and H. Hage, *Chemical Physics Letters* **103**, 98 (1983).
- [87] W. Preuss and G. Baumgartner, *Zeitschrift fur Physik A Atoms and Nuclei* **320**, 125 (1985).
- [88] S. Rai, B. Hemmerling, and W. Demtröder, *Chemical Physics* **97**, 127 (1985).
- [89] X. Xie and R. W. Field, *The Journal of Chemical Physics* **83**, 6193 (1985).
- [90] X. Xie and R. W. Field, *Chemical Physics* **99**, 337 (1985).
- [91] S. F. Rice, X. Xie, and R. W. Field, *Chemical Physics* **104**, 161 (1986).
- [92] S. F. Rice and R. W. Field, in *Methods of Laser Spec-troscopy*, edited by Y. Prior, A. Ben-Reuven, and M. Rosenbluh (1986) pp. 389–398.
- [93] L. Li, T. An, T.-J. Whang, A. M. Lyyra, W. C. Stwalley, R. W. Field, and R. A. Bernheim, *The Journal of Chemical Physics* **96**, 3342 (1992).
- [94] C. Linton, R. Bacis, P. Crozet, F. Martin, A. Ross, and J. Verges, *Journal of Molecular Spectroscopy* **151**, 159 (1992).
- [95] L. Li, S. Antonova, A. Yiannopoulou, K. Urbanski, and A. M. Lyyra, *The Journal of Chemical Physics* **105**, 9859 (1996).
- [96] T. Weyh, K. Ahmed, and W. Demtröder, *Chemical Physics Letters* **248**, 442 (1996).
- [97] L. Li, S. Antonova, A. Yiannopoulou, P. Crozet, A. Ross, F. Martin, and C. Linton, *Journal of Molecular Spectroscopy* **184**, 129 (1997).
- [98] G. Lazarov, A. Lyyra, and L. Li, *Journal of molecular spectroscopy* **205**, 73 (2001).
- [99] A. N. Drozdova, A. V. Stolyarov, M. Tama-nis, R. Ferber, P. Crozet, and A. J. Ross, *Physical Review A* **88**, 022504 (2013).
- [100] A. N. Drozdova, W. Skomorowski, M. Musial, R. Gonzalez-Ferez, C. P. Koch, and R. Moszynski, *Molecular Physics* (2013).
- [101] J. Zaharova, M. Tamanis, R. Ferber, A. N. Drozdova, E. A. Pazyuk, and A. V. Stolyarov, *Physical Review A* **79**, 012508 (2009).
- [102] A. Kruzins, I. Klincare, O. Nikolayeva, M. Tama-nis, R. Ferber, E. A. Pazyuk, and A. V. Stolyarov, *Physical Review A* **81**, 042509 (2010).
- [103] O. Docenko, M. Tamanis, R. Ferber, T. Bergeman, S. Kotochigova, A. V. Stolyarov, A. de Faria Nogueira, and C. E. S. F. de Souza, *Physical Review A* **81**, 042511 (2010).
- [104] J. Bai, E. H. Ahmed, B. Beser, Y. Guan, S. Kotochigova, A. M. Lyyra, S. Ashman, C. M. Wolfe, J. Huennekens, A. N. Drozdova, E. Pazyuk, A. V. Stolyarov, J. G. Danzl, H.-C. Nägerl, N. Bouloufa, O. Dulieu, C. Amiot, H. Salami, and T. Bergeman, *Physical Review A* **83**, 032514 (2011).
- [105] H. Harker, P. Crozet, A. J. Ross, K. Richter, J. Jones, C. Faust, J. Huennekens, A. V. Stolyarov, H. Salami, and T. Bergeman, *Physical Review A* **92**, 012506 (2015).
- [106] M. M. Hessel and C. R. Vidal, *The Journal of Chemical Physics* **70**, 4439 (1979).

- [107] I. Russier, F. Martin, C. Linton, P. Crozet, A. Ross, R. Bacis, and S. Churassy, *Journal of Molecular Spectroscopy* **168**, 39 (1994).
- [108] N. Bouloufa, P. Cacciani, R. Vetter, and A. Yiannopoulou, *The Journal of Chemical Physics* **111**, 1926 (1999).
- [109] P. Cacciani and V. Kokoouline, *Physical Review Letters* **84**, 5296 (2000).
- [110] N. Bouloufa, P. Cacciani, V. Kokoouline, F. Masnou-Seeuws, R. Vetter, and L. Li, *Physical Review A* **63**, 042507 (2001).
- [111] N. Bouloufa, P. Cacciani, R. Vetter, A. Yiannopoulou, F. Martin, and A. J. Ross, *The Journal of Chemical Physics* **114**, 8445 (2001).
- [112] R. A. Bernheim, *The Journal of Chemical Physics* **76**, 57 (1982).
- [113] B. Barakat, R. Bacis, S. Churassy, R. Field, J. Ho, C. Linton, S. Mc Donald, F. Martin, and J. Vergès, *Journal of Molecular Spectroscopy* **116**, 271 (1986).
- [114] C. Linton, F. Martin, R. Bacis, and J. Vergès, *Journal of Molecular Spectroscopy* **142**, 340 (1990).
- [115] M. Kubkowska, A. Grochola, W. Jastrzebski, and P. Kowalczyk, *Chemical Physics* **333**, 214 (2007).
- [116] R. F. Barrow, N. Travis, and C. V. Wright, *Nature* **187**, 141 (1960).
- [117] K. Ishikawa, S. Kubo, and H. Kato, *The Journal of Chemical Physics* **95**, 8803 (1991).
- [118] A. Ross, P. Crozet, C. Linton, F. Martin, I. Russier, and A. Yiannopoulou, *Journal of Molecular Spectroscopy* **191**, 28 (1998).
- [119] S. Kasahara, P. Kowalczyk, M. H. Kabir, M. Baba, and H. Kato, *The Journal of Chemical Physics* **113**, 6227 (2000).
- [120] D. A. Miller, L. P. Gold, P. D. Tripodi, and R. A. Bernheim, *The Journal of Chemical Physics* **92**, 5822 (1990).
- [121] R. A. Bernheim, *The Journal of Chemical Physics* **74**, 2749 (1981).
- [122] R. A. Bernheim, L. P. Gold, P. B. Kelly, C. Kittrell, and D. K. Veirs, *Physical Review Letters* **43**, 123 (1979).
- [123] R. Bernheim, L. Gold, and T. Tipton, *Chemical Physics Letters* **92**, 13 (1982).
- [124] L. Li, G. Lazarov, and A. Lyyra, *Journal of Molecular Spectroscopy* **191**, 387 (1998).
- [125] G. Lazarov, A. Lyyra, and L. Li, *Journal of molecular spectroscopy* **205**, 73 (2001).
- [126] X. Dai, E. A. Torres, E.-B. W. Lerch, D. J. Wilson, and S. R. Leone, *Chemical Physics Letters* **402**, 126 (2005).
- [127] X. Xie and R. W. Field, *The Journal of Chemical Physics* **83**, 6193 (1985).
- [128] X. Xie and R. Field, *Journal of Molecular Spectroscopy* **117**, 228 (1986).
- [129] C. Linton, F. Martin, A. Ross, I. Russier, P. Crozet, A. Yiannopoulou, L. Li, and A. Lyyra, *Journal of molecular spectroscopy* **196**, 20 (1999).